

**A comparative study of gemini surfactants 16-3-16 and  
16-7NH-16 as possible microbubble gene carriers**

by

Stephanie Schaefer

A thesis  
presented to the University of Waterloo  
in fulfillment of the  
thesis requirement for the degree of  
Master of Science  
in  
Biology

Waterloo, Ontario, Canada, 2010

©Stephanie Schaefer 2010

## **AUTHOR'S DECLARATION**

I hereby declare that I am the sole author of this thesis. This is a true copy of the thesis, including any required final revisions, as accepted by my examiners.

I understand that my thesis may be made electronically available to the public.

## Abstract

Gene therapy holds great promise to treat a variety of human diseases, including diabetes. The development of a new gene delivery system called Ultrasound Targeted Microbubble Destruction (UTMD) has been developed to enhance *in vivo* gene delivery using non-viral vectors. A new family of cationic lipids called gemini surfactants have been synthesized for their use as gene carriers due to their small particle size, increased surface charge, superior surface binding capabilities, reduced toxicity, and economic advantages, resulting in their increased safety for *in vivo* application. Gemini surfactants have not been evaluated with UTMD. The purpose of this study was to assess their transfection capabilities as microbubble gene carriers.

First, gemini surfactants 16-3-16 and 16-7NH-16 were assessed and compared to three commercially used monovalent cationic lipids: 1) Lipofectamine 2000, 2) Fugene, and 3) DOTAP microbubbles. Colloidal stability was assessed using dynamic light scattering to measure size and electrophoresis for charge. Gemini surfactants 16-3-16 and 16-7NH-16 displayed a small particle size of 2.33  $\mu\text{m}$  (16-3-16), 0.74  $\mu\text{m}$  (16-7NH-16) and increased surface charge of +34.8 mV (16-3-16), +37.74 mV (16-7NH-16) when compared to commercially used monovalent cationic lipid Lipofectamine 2000 (size 3.9  $\mu\text{m}$  and charge -6.2 mV). Gemini surfactant 16-7NH-16 was chosen for further investigation due to its reduced particle size and increased surface charge and was investigated for its DNA binding and release capabilities using UTMD through gel electrophoresis. Gel electrophoresis analysis determined gemini surfactant 16-7NH-16 was capable of fully binding 25  $\mu\text{g}$  of pAMAXA plasmid GFP DNA, but not able to release DNA when exposed to ultrasound. Transfection efficiency of gemini surfactant 16-7NH-16 microbubbles with 25  $\mu\text{g}$  of pAMAXA plasmid GFP DNA was additionally investigated in HEK 293 (human embryonic kidney cells) and INS-1 832/13 cells (rat insulinoma cells) using UTMD, and determined with fluorescent microscopy. Gemini surfactant 16-7NH-16 microbubbles resulted in a 5 % transfection rate and a 90 % death rate *in vitro* when exposed to UTMD. Commercially used monovalent cationic lipid microbubbles exhibited higher transfection rates and lower death rates overall *in vitro* when compared to gemini surfactant 16-7NH-16 microbubbles and exposed to UTMD. (Lipofectamine 2000 70 % transfection rate, 5 % death rate, Fugene 70 % transfection rate, 5 % death rate, DOTAP 30 % transfection rate, 90 % death rate). Cationic lipid microbubbles most influenced *in vitro* using the UTMD technique for transfection was DOTAP in combination with neutral lipids (DOTAP + neutral lipids). Transfection rates of DOTAP + neutral lipids increased as ultrasound intensities increased (10 % transfection at intensity 1.5  $\text{W}/\text{cm}^2$  and 30 % transfection at intensity 2.0  $\text{W}/\text{cm}^2$ ), demonstrating a direct correlation. *In vitro* gene delivery demonstrated gemini surfactant 16-7NH-16 microbubbles did not significantly enhance transfection capabilities when incorporated with the UTMD technique when compared to commercially used monovalent cationic lipids. Cationic lipid microbubble most influenced by ultrasound was DOTAP + neutral lipid microbubbles when compared to all experimental groups tested with the UTMD technique.

These results indicate that gemini surfactants, a new family of cationic lipids could not significantly enhance cellular transfection rates *in vitro* with the incorporation of the UTMD technique; despite their small particle size, increased surface charge, superior surface binding capabilities and economic advantage for *in vivo* application when compared to commercially used cationic monovalent lipids.

## Acknowledgements

I would like to take this time to not only acknowledge but to thank all the people who made this project possible. Firstly, I would like to thank my committee members Dr. Bernard Dunker, Dr. Jamie Joseph, Dr. David Spafford, and Dr. Russ Tupling, for all of their help, support, and guidance though out the past two years.

Jamie, I would like to take this time to personally thank you for taking me on as your first master's student, and giving me such wonderful opportunities in your lab.

Thanks to my family. Mom, you are my hero and have supported me every step of the way. You never gave up faith in me no matter how many times I told myself I couldn't. You mean the world to me and I hope one day to be just as strong of a woman as you. I love you and I am so proud to say that you are my mom and I look up to you more than anyone on this planet. Thanks to my loving sister Meredith. Meredith, I love you with all of my heart and soul! I would have never gotten though any of this without you! Thanks for listening to me and talking me though all of the tough times; I know you will miss listening to all of my stories. And thank you to my brother Matt. Matt, you are the best brother a sister could have. Thank you for all of your support. I know you can relate to all of my experiences.

I would also like to acknowledge some of the most supportive and important people who really help made this happen for me. Thanks to the most amazing lab team! Tanya Sheinin THANK YOU! I will never forget you. You helped me every inch of the way, teaching and supporting me in all I did in the lab. Renjitha Pillai, what a journey this has been. Thanks for your loving support. Mei Huang, Mei you too will be deeply missed. Mei you could always put a smile on my face! You could always say the right thing at the right time to make my day that much brighter. And last but certainly not least Dr. Peter Huypens. Peter I would like to send out a special thanks to you. Peter as I always said, you are a blessing. It is because of you my confidence grew. And I cannot thank you enough for spending so much of your time with me. I have never received such support and compassion from a person. Working with you was the most life changing experience. You are my mentor, a true scientist and a man I will look up to for the rest of my life. Thanks for always believing in me even in moments when I did not believe in myself. You have changed my life in ways you will never know. I will NEVER forget you!

Thank you to my committee members, Dr. Jamie Joseph, and the Joseph team for making all of this possible.

Sincerely,

Stephanie Schaefer

## **Dedication**

I would like to dedicate this Master's thesis in memory of my father. Dr. John Charles Schaefer. Dad you are my inspiration. Although you are not here to see me graduate there is no doubt in my mind that you are always by my side. It is your spirit that surrounds me at all times and encourages me never to give up. I miss you so much dad, but one day I will see you again. I hope your little princess has made you proud.

## Table of Contents

Author's Declaration .....	ii
Abstract .....	iii
Acknowledgements .....	v
Dedication .....	vi
Table of Contents .....	vii
List of Figures.....	x
List of Abbreviations.....	xii
Chapter 1 .....	1
1.1 Gene Therapy .....	1
1.2 Definition and Etiology of Diabetes Mellitus.....	1
1.3 Anatomy of the Islets of Langerhans.....	2
1.4 Mechanism of Insulin Secretion .....	4
1.5 ATP-Sensitive Potassium Channel ( $K^+_{ATP}$ ) Dependent Pathway.....	4
1.1 ATP-Sensitive Potassium Channel ( $K^+_{ATP}$ ) Independent Pathway .....	7
Chapter 2 .....	11
2.1 Prevention & Treatment Strategies for Diabetes.....	11
2.2 Prevention.....	11
2.3 Treatment.....	11
2.4 Self- Monitoring of Blood Glucose (SMBG).....	11
2.5 Artificial Pancreas .....	12
2.6 Islet Transplantation .....	12
Chapter 3 .....	14
3.1 Viral gene-delivery .....	14
3.1 Non-Viral Gene Delivery .....	15
3.2 Cationic Lipids .....	15
3.3 Gemini Surfactants .....	19

3.4 Colloidal Stability Measured Through Zeta Potential .....	24
3.5 Cationic Lipids for Drug and Gene Delivery .....	24
3.6 Ultrasound Targeted Microbubble Destruction .....	26
3.7 Microbubbles .....	26
3.8 UTMD Delivery Mechanism.....	27
3.9 UTMD and its In Vivo Application.....	30
3.10 UTMD as a tool for diabetes treatment .....	31
Purpose .....	32
Objective 1: Optimization of a Microbubble Gene Carrier.....	32
Objective 2: In Vitro Assessment of Optimized Microbubble Gene Carrier .....	33
Objective 3: Assess UTMD DNA release.....	33
Chapter 4 .....	34
4.1 Methods .....	34
Plasmid DNA Synthesis .....	34
Synthesis of Cationic Lipid Stocks.....	34
Synthesis of Microbubbles .....	35
Displacement of the Aqueous Center.....	35
Particle Size and Charge .....	35
Gemini Surfactant pAMAXA Plasmid DNA Binding Analysis through Electrophoresis gel.....	36
Plasmid DNA Binding and Release using UTMD .....	36
Chapter 5 .....	37
5.1 Results .....	37
5.2 Optimization of a Microbubble Gene Carrier.....	37
Assessing Gemini Surfactant Particle Size.....	37
Particle Surface Charge Analysis through Zeta Potential .....	39
Plasmid pAMAXA GFP DNA binding effects on particle size .....	41
Plasmid pAMAXA GFP DNA binding effects on zeta potential.....	43



Plasmid pAMAXA GFP DNA binding analysis of gemini surfactant 16-7NH-16 through gel electrophoresis .....	45
5.3 In Vitro Assessment of Optimized Microbubble Gene Carrier .....	47
Assessing ultrasound transfection capabilities in attached HEK 293 cells .....	47
Assessing ultrasound cell viability after transfection in attached HEK 293 cells .....	49
Assessing ultrasound transfection capabilities in suspended HEK 293 cells .....	51
Assessing ultrasound cell viability after transfection in suspended HEK 293 cells .....	53
Assessing ultrasound transfection capabilities of INS-1 832/13 cells in suspension .....	55
Assessing ultrasound cell viability after transfection in suspended INS-1 832/13 cells .....	57
Assessing plasmid pAMAXA GFP DNA binding and release using ultrasound .....	59
Chapter 6 .....	63
6.1 Discussion .....	63
Bibliography .....	73

## List of Figures

Figure 1: Illustration of the human pancreas including islets of Langerhans .....	3
Figure 2: Glucose-Stimulated Pathway of Insulin Secretion. ....	6
Figure 3: ATP-sensitive potassium channel ( $K_{ATP}$ ) independent pathways.....	10
Figure 4: Structure of a Monovalent Cationic Lipid. ....	16
Figure 5: Structures Formed by Cationic Lipids Suspended in Solution.....	18
Figure 6: Structure of a Gemini Surfactant Cationic Lipid.....	21
Figure 7: Chemical Structure of Gemini Surfactants Exhibiting Different Spacer Groups.....	23
Figure 8: Ultrasound Targeted Microbubble Destruction. ....	28
Figure 9: Particle size comparison of cationic gemini surfactants 16-3-16, 16-7NH-16, and Lipofectamine 2000 Microbubbles .....	38
Figure 10: Zeta potential comparison of cationic gemini surfactants 16-3-16, 16-7NH-16, and Lipofectamine 2000 Microbubbles .....	40
Figure 12: Particle size comparison of cationic gemini surfactants with and without the addition of plasmid pAMAXA GFP DNA.....	42
Figure 13: Zeta potential comparison of gemini surfactants 16-3-16 and 16-7NH-16 with and without the addition of plasmid pAMAXA GFP DNA: .....	44
Figure 14: Gemini surfactant plasmid DNA binding analysis through gel electrophoresis.....	46
Figure 15: Transfection efficiency comparison of pAMAXA plasmid GFP in attached HEK 293 cells using ultrasound .....	48
Figure 16: Cell viability of transfected HEK 293 cells using ultrasound .....	50
Figure 17: Transfection efficiency comparison of pAMAXA plasmid GFP in suspended HEK 293 cells using ultrasound .....	52
Figure 18: Cell viability of transfected HEK 293 cells in suspension using ultrasound.....	54
Figure 19: Transfection efficiency comparison of pAMAXA plasmid GFP in suspended INS-1 832/13 cells using ultrasound.....	56
Figure 20: Cell viability of transfected INS-1 832/13 cells in suspension using ultrasound.....	58

Figure 21: Plasmid pAMAXA GFP DNA binding and release with ultrasound. ....60  
Figure 22: Ultrasound Mediated Destruction of Neutral Gas Filled Microbubbles.....62

## List of Abbreviations

ADP: Adenosine diphosphate  
ATP: Adenosine-5'-triphosphate  
CIC: Citrate/Isocitrate Carrier  
CL: Citrate lyase  
DAG: Diacylglycerol  
DNA: Deoxyribonucleic acid  
DNase: Deoxyribonuclease  
DOPE: L- $\alpha$ -Phosphatidylethanolamine, dioleoly  
DOTAP: 1,2-dioleoyl-3-trimethylammonium-propane  
DPPC: DL- $\alpha$ -Phosphitdylcholine, Dipalmitoyl (DPPC)  
GSIS: Glucose Stimulated Insulin Secretion  
HEK Cells: Human Embryonic Kidney Cells  
HEPES: N-(2-Hydroxyethyl)piperazine-N'-(2-ethanesulfonic acid)  
ICDc: Isocitrate dehydrogenase  
INS-1 832/13: Rat insulinoma cells  
MB: Microbubbles  
MODY: Maturity Onset Diabetes of the Young  
NAD: Nicotinamide adenine dinucleotide  
NADP: Nicotinamide adenine dinucleotide phosphate  
NADPH: Nicotinamide adenine dinucleotide phosphate  
PBS: Phosphate Buffered Saline  
PC: Pyruvate Carboxylase  
PDH: Pyruvate Dehydrogenase  
RIP: Rat insulin 1 promoter  
RNA: Ribonucleic acid  
TCA cycle: Tricarboxylic Acid Cycle  
VDCC: Voltage-gated Ca<sup>2+</sup> Channels

VEGF: Vascular Endothelial Growth Factor

UTMD: Ultrasound Targeted Microbubble Destruction

# Chapter 1

## 1.1 Gene Therapy

Gene therapy is a new therapeutic concept proposed to treat a variety of human diseases. In most cases, a disease is a result of the misregulation or expression of a particular gene (Heilbronn et al., 2010; Karp et al., 2003). This disruption in gene expression can cause an imbalance in biological processes within a cell, resulting in disease. The goal or objective of gene therapy is to deliver nucleic acids, either RNA or DNA, into a target cell in order to modify its function (Heilbronn et al., 2010; Karp et al. 2003; Robbins et al., 1998). This process involves the addition, deletion or the alteration of a specific gene(s) in a target cell (Karp et al., 2003; Robbins et al., 1998). Diabetes *mellitus*, commonly known as diabetes, is a human disease whose global epidemic is on the rise. Gene therapy holds great promise for its medical application as a new treatment for this disease.

## 1.2 Definition and Etiology of Diabetes Mellitus

Diabetes is a life altering chronic disease. Diabetes occurs when insulin production from pancreatic  $\beta$ -cells is impaired and unable to meet the metabolic demands of peripheral tissues (Oliver-Krasinski et al., 2008; Pfeifer et al., 1981; Newsholme et al., 2010). There are two forms of diabetes, type 1 and type 2; both forms occur as a result of the impairment in  $\beta$ -cell function and mass leading to hyperglycemia (Oliver-Krasinski et al., 2008; Taplin et al., 2008; Castano et al., 1990; Ferrannini et al., 1998).

Type 1 diabetes is classified as an autoimmune disease resulting from the immune-mediated loss of insulin-secreting  $\beta$ -cells. The immune system of type 1 diabetics develops auto-antibodies which both selectively target and destroy the insulin producing  $\beta$ -cells of the pancreas (Ziegler, et al., 2010; Taplin et al., 2008). Type 2 diabetes differs from type 1 as it is not due to the misregulation of the immune system, but rather is linked to obesity. Type 2 diabetes is characterized by abnormal  $\beta$ -cell function, but not complete insulin deficiency. Type 2 diabetics still have the ability to secrete insulin, but there is a malfunctioning in secretion leading to indiscriminate blood glucose levels (Stock et al., 2004; Stagner et al., 1992; Rahier et al., 2008; Szabadkai, et al. 2009).

### 1.3 Anatomy of the Islets of Langerhans

The human pancreas is known as both an endocrine and exocrine organ, and holds residence to the insulin producing  $\beta$ -cells. The bulk of the pancreas is composed of acinar cells. Acinar cells produce enzymes which are secreted and aid during digestion. Scattered among the acinar tissue are small clusters of cells known as islets of Langerhans (Marieb, et al., 2007; Samol et al., 1998). Islet cells are small circular clusters of approximately 1000 cells. Three cell types exist in islets, alpha  $\alpha$ , beta  $\beta$  and delta  $\delta$  cells. The orientation of these cells within an islet is important for cell signalling and communication to maintain appropriate blood glucose levels (Marieb, et al., 2007; Samols et al., 1986; Samol et al., 1998; Unger et al., 1978). The two major hormone producing cells of the pancreas are: alpha ( $\alpha$ ) and beta ( $\beta$ ) cells. Alpha cells are responsible for producing glucagon and  $\beta$ -cells insulin. It is the  $\beta$ -cells which are responsible for detecting a rise in blood glucose levels, and secreting insulin to restore normal blood glucose (Unger et al., 1978; Samol et al., 1986; Newsholmen et al., 2010). Glucose not only stimulates insulin secretion directly but also stimulates the production of free fatty acids, amino acids, and glucagon like peptide -1 (Jensen, et al., 2008). The  $\beta$ -cells of the pancreas are entwined within a delicate microvasculature to enable accurate detection of any rise in blood glucose levels (Brunicardi et al., 1996; Orci et al., 1975). A supportive extracellular matrix surrounds these cells which directly impacts  $\beta$ -cell function, survival and replication (Halban, et al., 2010; Bonner-Weir et al., 1994; Bonner-Weir et al., 2000). The  $\beta$ -cells of the pancreas require close coordination, tight control and tremendous communication from surrounding cells such as  $\alpha$  and  $\delta$  cells, to sustain adequate control to maintain normal glycaemic conditions (Figure 1) (Marieb, et al., 2007; Samols et al., 1986; Bansal et al., 2008)

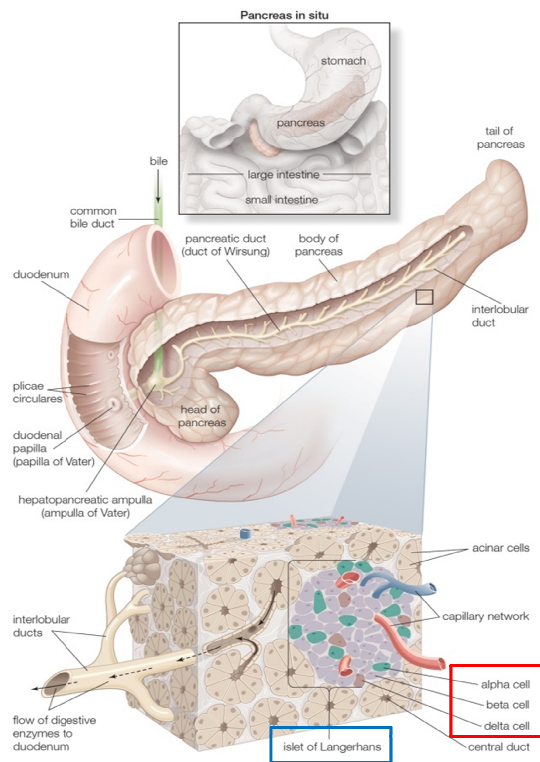


**Figure 1: Illustration of the human pancreas including islets of Langerhans:** This figure describes the location of the human pancreas, including the islets of Langerhans structure and vascularization. The human pancreas is located behind the stomach and is composed of both endocrine and exocrine tissue. The bulk of the pancreas is made up of exocrine tissue, forming acinar cells. Acinar cells produce enzymes which aid in the digestion of food. Spread though out the exocrine tissue are pancreatic islets, also known as the islets of Langerhans (indicated by the blue box). Islets of Langerhans are tiny cell clusters of approximately 1000 cells which produce pancreatic hormones. The three main hormone producing cells of an islet are  $\alpha$ ,  $\beta$ , and  $\delta$ -cells (indicated by the red box).  $\alpha$ -cells produce the hormone glucagon and prevent hypoglycemia,  $\beta$ -cells produce the hormone insulin preventing hyperglycemia. Islets of Langerhans are highly vascularized cellular structures to allow tight control over the rising and lowering of blood glucose levels. Marieb, E., (2007). Anatomy & Physiology, seventh edition, San Francisco: Pearson Education



## **1.4 Mechanism of Insulin Secretion**

The absolute mechanism and regulation of insulin secretion from pancreatic  $\beta$ -cells is not completely understood; although, studies have well established that insulin secretion from  $\beta$ -cells occurs in a biphasic fashion in response to a rise in blood glucose (Gembal, et al., 1992; Sato et al., 1992; Wang et al., 2009; Hou et al., 2009; Straub et al., 2002). Pancreatic  $\beta$ -cells have the capacity to sense a rise in blood glucose levels and produce insulin through several insulin secreting pathways. The most intensively investigated pathway is the glucose stimulated pathway of insulin secretion (MacDonald et al., 2005; MacDonald et al., 1995, MacDonald et al., 1993; Ronnebaum et al., 2005; Ronnebaum et al., 2006).

The metabolism of glucose plays a key role in regulating insulin release. As glucose levels in the blood begin to raise after a meal, a cascade of events occur resulting in insulin secretion (Mears et al., 2004; Henquin et al., 2009; Newsholme et al., 2010). Glucose from the blood enters the islet cell microcirculation, here pancreatic  $\beta$ -cells respond to increasing extracellular glucose levels in a biphasic pattern. The first phase lasts approximately ten minutes and results in a quick burst or spike in insulin secretion that declines rapidly after ten minutes. The second phase of insulin secretion consists of a steady, slow increase until reaching a plateau after approximately thirty minutes (Mears et al 2004; Straub et al., 2002; Wang et al., 2009; Nesher et al., 2002).

## **1.5 ATP-Sensitive Potassium Channel ( $K_{ATP}^+$ ) Dependent Pathway**

The intracellular mechanism of insulin secretion in response to glucose involves several steps. First, glucose enters the  $\beta$ -cell through the glucose transporter 2 (GLUT 2), and initiates glycolysis. The end product of glycolysis is the production of two pyruvate molecules, NADH and ATP (MacDonald et al., 2005; MacDonald et al., 1995; Henquin et al., 2009; Newsholme et al., 2010). As ATP molecules are produced they bind to the  $K_{ATP}$  channel leading to a rise in the cytosolic ATP:ADP ratio. The increase in ratio of ATP:ADP leads to the closure of the  $K_{ATP}$

channel and the depolarization of the plasma cell membrane (Jacobson et al., 2007; Jitrapakdee et al., 2010; Jensen et al., 2008; MacDonald et al., 1995). The depolarization of the  $\beta$ -cell plasma membrane results in the activation of the voltage-gated L-type  $\text{Ca}^{2+}$  channels that causes an influx of  $\text{Ca}^{2+}$  into the cytosol. As  $\text{Ca}^{2+}$  concentrations increase inside the cell, it signals the exocytosis of the immediately releasable pool (IRP) of insulin granules (Henquin et al., 2009; MacDonald et al., 2005; Mears et al., 2004; Wang et al., 2009; Jitrapakdee et al., 2010). This first acute phase of insulin secretion is known as the  $\text{K}_{\text{ATP}}$  channel dependent pathway and its role has been well established (Figure 2).

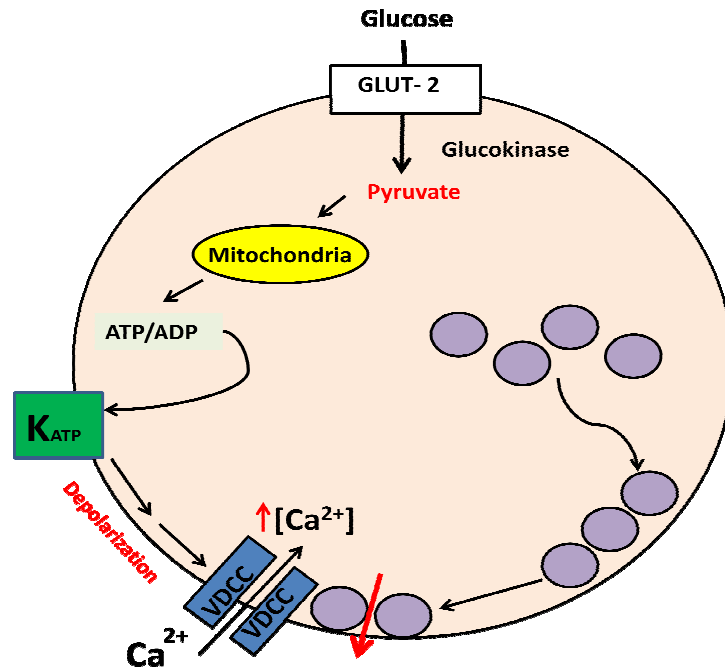


**Figure 2: Glucose-Stimulated Pathway of Insulin Secretion:** Schematic representing the channels and steps involved in the triggering and metabolic pathways mediating the stimulation of insulin secretion by glucose. First, glucose enters the  $\beta$ -cells through the glucose transporters (GLUT-1 in humans; GLUT-2 in rodents). Glucose is transported into the cells cytosol and glycolysis begins. Glucose is phosphorylated by the enzyme glucokinase to produce two pyruvic acid molecules. Pyruvate enters the mitochondrion where it is decarboxylated producing the rapid production of reducing equivalents by the TCA cycle. These reducing equivalents are further oxidized in the respiratory chain enabling ATP production. ATP is shuttled to the cytoplasm where there is an increase in the ATP: ADP ratio. This increased ratio promotes the closure of the ATP-sensitive  $K^+$  ( $K_{ATP}$ ) channel depolarizing the cellular membrane. The depolarized cellular membrane signals the activation of the voltage-gated (VDCC)  $Ca^{2+}$  channels.  $Ca^{2+}$  rushes inside the cells cytosol increasing the intercellular concentration of  $Ca^{2+}$  triggering the exocytosis of insulin granules into the blood stream.

## 1.1 ATP-Sensitive Potassium Channel ( $K^+_{ATP}$ ) Independent Pathway

The idea of another possible pathway involved in insulin secretion has been determined (Pantel et al., 1988; Wiederkehr et al., 2009, Henquin et al., 2009). This pathway is known as the  $K_{ATP}$  channel independent pathway and is the result of the second or more sustained phase of the biphasic pattern during insulin secretion (Gembal, et al., 1992; Sato et al., 1992). The identification of a second pathway was determined through two independent studies. The first study investigated insulin secretion by applying sulfonylureas drugs to  $\beta$ -cells. Sulfonylureas mimic glucose stimulation by acting directly on membrane potential and  $Ca^{2+}$  influx, by closing the  $K_{ATP}$  channels independently of changes in metabolism. In this study,  $\beta$ -cells were bathed in high concentrations of glucose at 15 mmol/L, which induced a higher rate of insulin secretion when compared to 10 mmol/l and 5  $\mu$ mol/l of the sulfonylureas drug tolbutamide. It was therefore proposed that non-electrical effects of glucose amplify insulin secretion (Henquin, et al., 1998; Henquin et al., 2000). A second study determined glucose is able to increase insulin secretion in the presence of sulfonylurea concentrations sufficient to close all  $K_{ATP}$  channels in  $\beta$ -cells, also leading to the same conclusion that glucose is acting on other targets resulting in insulin secretion (Henquin et al., 2009; Henquin et al., 2000; Gembal, et al., 1992; Sato et al., 1992). Two more studies investigated this hypothesis and demonstrated that glucose can increase insulin secretion in the presence of diazoxide. Diazoxide acts as a clamp to hold open the potassium channels preventing the influx of  $Ca^{2+}$ . This effect demonstrated the important role metabolism plays during insulin secretion and required to elevate concentrations of  $Ca^{2+}$ . This pathway of insulin secretion has been termed the “metabolic amplifying pathway” (Nenquin et al., 2004; Henquin et al., 2000; Henquin 2003; Hellman et al., 1994; Ashcroft et al., 1989; Prentki et al., 1987; Cook et al., 1984; Dean et al., 1970). This has led to its investigation to fully understand the mechanisms of insulin secretion at the level of metabolism.

When describing the first phase of insulin secretion, the end product of glycolysis is pyruvate in  $\beta$ -cells. During metabolism, pyruvate is shuttled from the cytosol of the cell into the mitochondria where it enters into the tricarboxylic acid (TCA) cycle via pyruvate dehydrogenase (PDH) and

pyruvate carboxylase (PC). Here, pyruvate is shuttled at an equal magnitude and is either converted into acetyl-coenzyme A or oxaloacetate. It is these two substrates which are the beginning of the anaplerotic pathway resulting in new intermediate metabolites into the TCA cycle (Jensen, M., et al., 2008; Henquin et al., 2003; Maechler et al., 1997). Anabolic pathways lead to the production of more complex compounds that are generated from simple starting molecules (Karp et al., 2003). After the initial breakdown of pyruvate, three possible pyruvate cycling pathways are introduced, pyruvate/malate, pyruvate/citrate, and the pyruvate/isocitrate cycle (Jensen, M., et al., 2008; Joseph et al., 2006; Lue et al., 2002, MacDonald et al., 1995; Ogawa et al., 1995; Ronnebaum et al., 2006).

The first possible pathway is termed the pyruvate/malate pathway. This pathway begins by the generation of oxaloacetate from the pyruvate enzyme PC. This pathway involves the conversion of oxaloacetate to malate by the mitochondrial malate dehydrogenase enzyme. Once converted, malate is exported from the mitochondrion by the dicarboxylate malate carrier also known as DIC. Once present inside the cytosol, malate is then converted back to pyruvate by the malic enzyme resulting in the generation of NADPH, and shuttled back into the mitochondrion for further pyruvate cycling (Jensen et al., 2008; MacDonald et al., 1995; Henquin et al., 2003; Maechler et al., 1997) (Figure 3).

The second possible pathway is the pyruvate/citrate pathway, and involves the conversion of oxaloacetate to citrate. Citrate can follow two paths, either moved outside of the mitochondria by the citrate/isocitrate carrier (CIC), or is further broken down to form isocitrate. If citrate is shuttled outside the mitochondria into the cytosol, it is cleaved to form oxaloacetate or acetyl-CoA by the ATP-citrate lyase (CL) enzyme. This cleavage can result in the returning of pyruvate back into the mitochondria by the malic enzyme generating more NADPH (Jensen et al., 2008; Joseph et al., 2006; Lue et al., 2002, MacDonald et al., 1995; Ogawa et al., 1995; Ronnebaum et al., 2006) (Figure 3).

The last possible pathway is the pyruvate/isocitrate pathway, and involves the export of citrate and isocitrate from the mitochondria to the cytosol of the cell through the CIC carrier. Isocitrate then serves as a substrate for the NADP<sup>+</sup>-dependent isocitrate dehydrogenase (ICDc) generating NADPH and 2-oxoglutarate which can re-enter the TCA cycle or can be converted into  $\alpha$ -ketoglutarate and later producing glutamate which has been proposed to be an additive factor in the metabolic amplifying pathway (Figure 3) (Newsholme, et al. 2010; Fallon et al., 2008; Jensen, M., et al., 2008 Joseph et al., 2006; Lue et al., 2002, MacDonald et al., 1995; Ogawa et al., 1995; Ronnebaum et al., 2006).

Subsequently, glucose metabolism within the mitochondria generates metabolic coupling factors ultimately involved in the signaling for insulin secretion (Newsholme, et al. 2010; Henquin et al., 2009; Boucher et al., 2004; Jeffrey et al., 1996; Lue et al., 2002; Newgard et al., 1995).

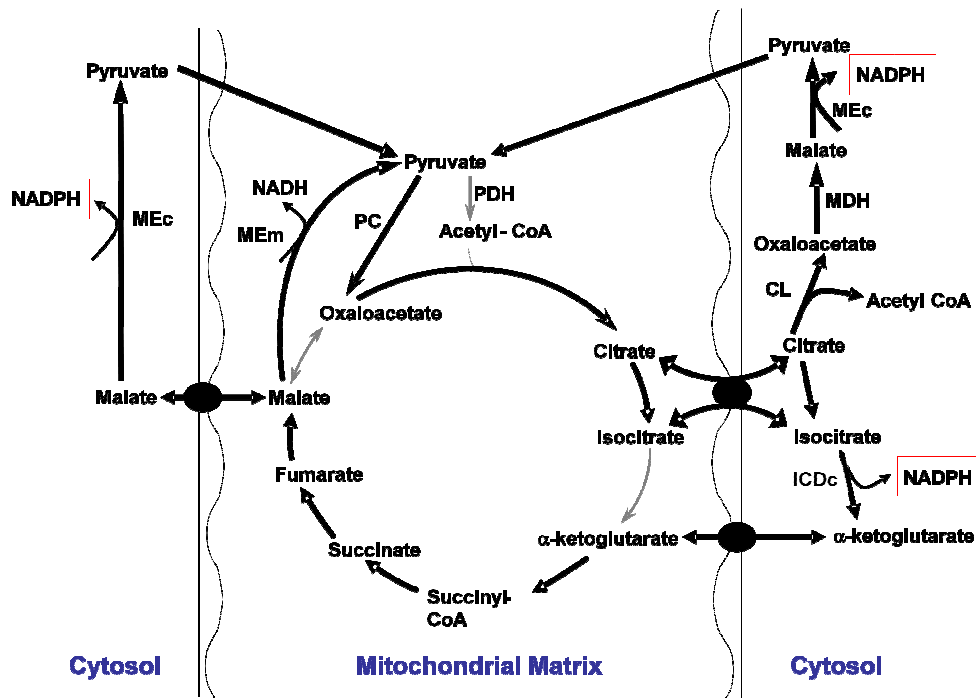


**Figure 3: ATP-sensitive potassium channel ( $K_{ATP}$ ) independent pathways:** This figure illustrates the TCA cycle and three putative pyruvate cycling pathways which are considered to augment insulin secretion via the production of cytosolic NADPH. Reference: MacDonald, 2002, Modified by Dr. Jamie Joseph and Stephanie Schaefer

# Chapter 2

## **2.1 Prevention & Treatment Strategies for Diabetes**

### **2.2 Prevention**

Type 2 diabetes makes up 90-95% of all diabetic cases. Several studies have provided strong correlation between the occurrence of type 2 diabetes and obesity, lack of exercise, an unhealthy life style, poverty and a low education background (Creatore et al., 2010; Rahier et al., 2008; Colom et al., 2010). These correlative studies, suggest that type 2 diabetes can be prevented or even cured by taking on a healthy lifestyle. However, for a minority (approximately 5%) of the type 2 diabetics, referred to as maturity onset diabetes of the young (MODY), a change in life style will not alter anything as this form of diabetes is caused by a single mutation in a number of genes such as GK, HNF1-alpha, HNF4-alpha, IPF1 (Pdx1), KLF11 (Colom et al., 2010).

### **2.3 Treatment**

Currently, there is no cure for diabetes. Secondary complications associated with the disease are of major concern. Unfortunately, existing therapies fail to provide adequate control over keeping blood glucose levels under control urging the need for a more effective and long-lasting treatment for diabetes (Halban et al., 2010).

### **2.4 Self- Monitoring of Blood Glucose (SMBG)**

Self-monitoring of blood glucose (SMBG) did not become available until the 1940's, until then blood glucose monitoring was an extensive laboratory process. The first self-assessment of blood glucose was performed by measuring the total reducing substances present in the urine. It wasn't



until the 1970's that self-monitoring of blood glucose was performed using reagent strips and a small drop of blood. This advancement in technology allowed hour to hour monitoring using a small volume of blood with only 10 % error. Drawbacks of this form of SMBG include: inconvenience, discomfort, secondary infections, repeated insulin injections and the risk of arriving at a hypoglycemic insult (Chee et al., 2004). With advancements in both research and technology, the development of the artificial pancreas began in 2003.

## **2.5 Artificial Pancreas**

The artificial pancreas has been developed in an attempt to increase the quality of life for people who suffer from diabetes. This device mimics the function of a normal pancreas as it consists of an implanted glucose monitoring device that is continuously supplied by the venous blood flow from the patient (Chee et al., 2004; Halban et al., 2010). The inclusion of a small computer and pump allows this system not only to perform “real time” measurements of the blood glucose levels, but also provides the means to ensure the release of accurate amounts of insulin at any given point in time. The main advantage of this system is the fact that the artificial pancreas relieves the patient from the tedious self-monitoring task and it ensures a tight normal glycemic control. However, several drawbacks including the need of invasive subcutaneous implantation, continuous calibration of the glucose sensing module, the increased chance for infection, blood clot formation as well as the irritation originating from sensor insertion site are the major limitations for the widespread use of this technology (Chee et al., 2004; Halban et al., 2010).

## **2.6 Islet Transplantation**

Islet transplantation is a strategy that aims to replenish the reduced  $\beta$ -cell mass in both MODY and type 1 diabetics by implanting islets from a deceased donor. Pancreatic islet transplantation became a successful method in the treatment of type 1 diabetes after the implementation of the Edmonton protocol, allowing a reduction in the number of islets that is required in the transplantation procedure but most significantly the use of glucocorticoid-free

immunosuppression post transplantation (Bretzel, et al. 2007; Yones et al., 2008; Shapiro et al., 2006; Shapiro et al., 2000). Nevertheless, the success of this method seems to be restrained by at least two major factors, including a limited islet supply and the need to use immunosuppressive drugs to ensure graft survival. It has been estimated that successful human islet transplantation requires at least 5000 islet equivalents per kilogram of body weight and can require up to three pancreatic donors, before the patient is no longer considered to be insulin-dependent (Shapiro et al., 2006; Yones et al., 2008). Although, the human islet isolation procedure has been standardized, islet yield continues to have a highly unpredictable and variable outcome (Kenmochi et al., 2008; Hara, et al., 2006; Yones et al., 2008; Halban et al., 2010).

Transplantation experiments in animals have demonstrated that approximately 50 % of the transferred islets will not engraft, and the clinical outcome of the transplantation procedure is negatively affected by the loss of functional capacity of the transplanted islets due to stress from the isolation and culture procedure, local inflammatory processes and/or the occurrence of hypoxia before revascularization is achieved (Bretzel et al., 2007; Yones et al., 2008; Halban et al., 2010). This poor graft survival has urged the need for an immunosuppressive regimen in the transplantation strategy which also encompasses a number of disadvantages for the patient, such as an increased risk of malignancy or life threatening infections. It should be noted that the long-term side effects of immunosuppressive medication are unknown. If the need for systemic immunosuppression could be significantly reduced, islet transplantation could be applied in the earliest stage of diabetes, during childhood. Several strategies, including gene therapy are currently being addressed in order to cope with the current limitations of islet transplantation and maintaining an insulin-independent status (Bretzel et al., 2007; Yones et al., 2008, Ludwig et al., 2010).

# Chapter 3

## 3.1 Viral gene-delivery

The most common delivery system for gene therapy is viral-mediated-gene transfer. Viral vectors are favored as gene delivery vehicles due to their easy production; high functioning titers and their ability to infect many different cell types (Mayer et al., 2008; Robbins et al., 1998). The most frequently used virus for gene delivery is the *Adenoviral* derived viruses (Feril et al., 2005). Gene therapy using viral vectors is achieved by integrating a target DNA sequence into the viruses' genome and exposing that virus to a target cell. The result is the desired gene integrated and expressed in a target cell (Roberts et al., 1998; Unger et al., 2001;). This form of gene therapy has been used for many treatments including cardiovascular disease of the myocardium and promotion of new blood vessels in ischemic tissue (Robbins et al., 1998; Unger et al., 2001;).

Gene therapy using viral vectors has been approved in human clinical trials. In 1989, the first human clinical trial was performed using viral vectors as gene delivery agents to treat cancer by inserting a gene into immune cells (Roberts et al., 1998). After this success, over 300 human clinical trials have been performed using viral vectors as gene delivery vehicles to treat disease (Roberts et al., 1998). However, many drawbacks exist when using viral vectors as a vehicle for gene therapy, such as: cytotoxicity, physical changes to the target cells, mediated mutagenesis of genomic DNA, and most importantly the ability to elicit an immune response (Robbins et al., 1998; Feril et al., 2005; Roberts et al., 1998). In 1995, a fatal accidental death occurred resulting from the use of *adenoviral* vectors for gene therapy through systemic administration. This death was the result of the over activation of innate immune system. This resulted in the re-evaluation of viral vectors as gene carriers in human trials (Roberts et al., 1998; Robbins et al., 1998).

### **3.1 Non-Viral Gene Delivery**

The strong inflammatory response initiated *in vivo* during gene delivery application using viral vectors has propelled research into the development of non-viral gene carriers whose clinical application can be deemed safe. When developing a non-viral gene delivery system several aspects must be considered. The delivery system must be capable of repeated administration with little to no immune response, low cost, stable at non-extreme conditions and easily administered to patients (Davis, et al., 2002; Gary et al., 2007). A new class of gene delivery agents called cationic lipids have been synthesized for this purpose.

### **3.2 Cationic Lipids**

Cationic lipids are positively charged phospholipids that readily bind and transfect DNA into a target cell. Two classes of cationic lipids exist, monovalent and a recently new family of cationic lipids called gemini surfactants. Structurally, cationic lipids are composed of a positively charged  $\alpha$ -amino acid head group and a hydrophobic fatty acid tail (Figure 4). The positively charged amino group is attached to its hydrophobic region by a linker; an example of a linker is glycerol (Tors et al., 2010; Rao et al., 2010). Transfection capabilities of cationic lipids depend on several structural factors. Such factors include the combination of the cationic amino head group, degree of the hydrophobic tails and the bond that links the hydrophobic tails (Yingyongnarongkul et al 2009; Rao et al., 2010). These structures can be very unstable; it is for this reasons that co-helper lipids are used. The most commonly used helper lipid is DOPE which helps structurally maintain the cationic lipid and increase transfection capabilities (Yingyongnarongkul et al 2009; Zhi et al., 2010; Zhdanov et al., 2002).

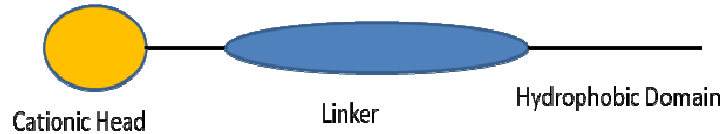


**Figure 4: Structure of a Monovalent Cationic Lipid:** Illustration of the basic structure of a monovalent cationic lipid used to deliver plasmid DNA both *in vivo* and *in vitro*. Cationic lipids are mainly composed of hydrophobic and hydrophilic regions. The positively charged amino acid head group is attached by what is known as a linker; an example of a linker is glycerol. This linker is attached to a hydrocarbon chain of fatty acids. Examples of monovalent cationic lipids are Lipofectamine 2000, Fugene, and DOTAP.

The hydrophobic domains of cationic lipids are very important in the self assembly of liposomes or microbubbles in the presence of helper lipids (Tranchant, et al. 2004). Cationic lipids have the capabilities to form various structures when suspended in solution. Some of the most common structures include the multilamellar, hexagonal, inverted hexagonal phase and spherical or liposomal structures (Figure 5) (Ma et al 2007). These structures have the ability to form spontaneously in solution. The type of structure formed is dependent upon the conditions in which lipids are developed such as: temperature, pH, the presence of other ions, and the ratio of lipids to DNA (Caracciolo et. al., 2005; Ma et al. 2007; Zhdanov et al., 2002). These factors will control the shape of the lipoplex. Lipids have the capabilities to shape shift during changing conditions. Research presented by Caracciolo et al., (2005) indicated that DC-CHol/DOPE-DNA complexes form a lamellar phase at temperatures ranging from 0-4°C, and these complexes have the ability to remain stable for up to three months.

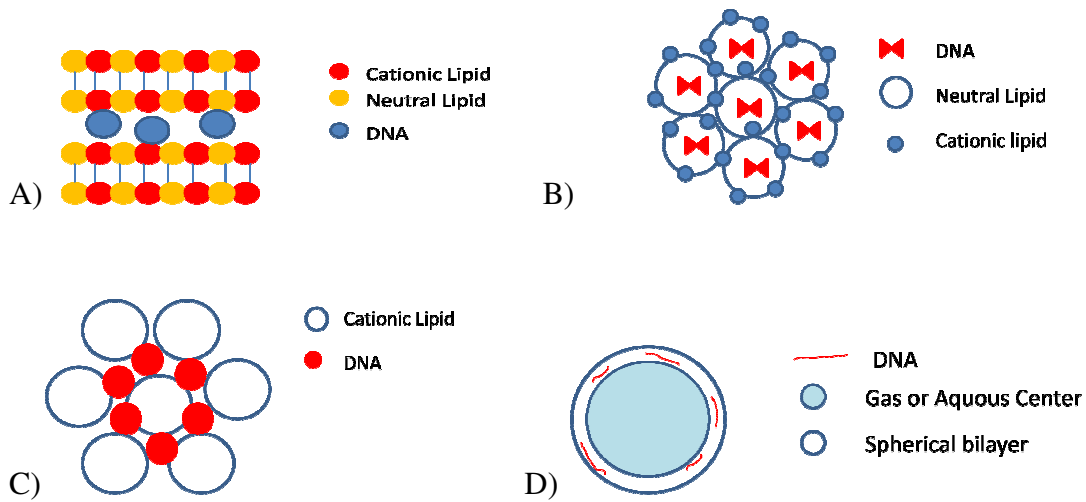


**Figure 5: Structures Formed by Cationic Lipids Suspended in Solution.** Illustration of the four possible structures cationic lipids can form A) lamellar structure, cationic lipid and DNA form a lipoplex, B) Inverted hexagonal lattice, C) Intercalated hexagonal structure, D) Spherical or liposomal structure composed of an aqueous or gas filled center with DNA sandwiched between the two bilayers.

Nucleic acids and cationic lipids spontaneously interact through electrostatic interactions (Zuhorn et al. 2002; Zhdanov et al., 2002; Wasungu et al., 2006). It is the spontaneous interaction between DNA and cationic lipids which form what is known as a lipoplex. These interactions with cationic lipids depend on factors such as incubation time with DNA, cationic lipid to helper lipid concentrations, and lipid to DNA ratios. Ultimately, these factors will have major impacts on the shape a lipoplex will form (Ma et al 2007; Rao et al., 2010).

Monovalent cationic lipids are the most commonly used, and have been shown to have high transfection capabilities; examples include Lipofectamine 2000, Fugene and DOTAP. Currently, more research has been focused on the design of cationic lipids in order to increase their DNA binding and transfection capabilities with reduced cellular toxicity. Recently, an extended amount of research has gone into the design of cationic lipids to increase DNA binding with superior surface binding capabilities, increased transfection, reduced toxicity, lower costs for economic advantages, and increased safety for *in vivo* application. A new family of cationic lipids called gemini surfactants have been created for these purposes (Kirby et al., 2003; Wettig, et al 2007; Wettig et al., 2008).

### **3.3 Gemini Surfactants**

Gemini surfactants are considered to be a relatively new class of cationic molecules. The structure of a gemini surfactant differs from the monovalent cationic lipid by the addition of a rigid spacer group (Figure 6). This additional spacer group increases surface DNA binding and packing capabilities 1000 times compared to the single chain, single head group of the monovalent cationic lipids (Kirby et al. 2003; Wettig et al., 2007; Wettig et al., 2008; Luciani et al., 2007). The increased DNA binding and packing capabilities demonstrated by gemini



surfactants reduce the amount of compound required for a successful transfection and increases their safety for *in vivo* application (Kirby et al., 2003; Ewert et al., 2002).

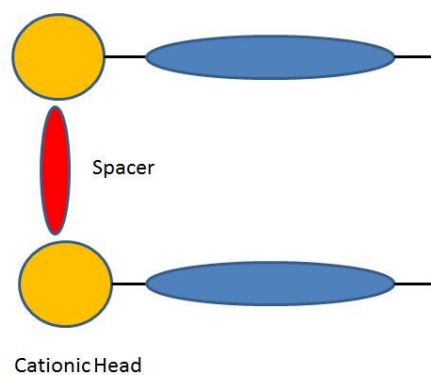
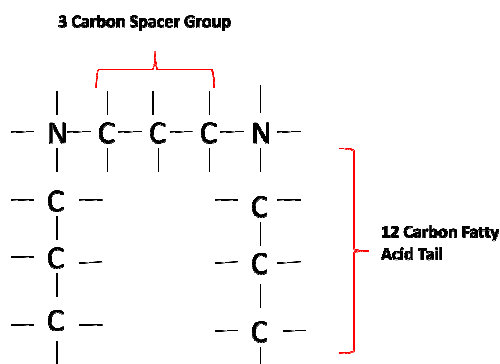


**Figure 6: Structure of a Gemini Surfactant Cationic Lipid.** Gemini surfactant cationic lipids differ from monovalent cationic lipids due to the addition of a ridged spacer group. The spacer group increases surface DNA association and packing capabilities. Examples of divalent cationic lipids are gemini surfactants 16-3-16 and 16-7NH-16.

The composition of the spacer chosen during the synthesis of gemini surfactants will depend upon the therapeutic agent being delivered. Several studies have investigated the effects that spacer length has on DNA binding and cellular transfection. Two commonly used spacers are the N-CH<sub>3</sub>, also known as *aza*, and the N-H *imino* group (Wettig, et al., 2008; Luciani et al., 2007).

Studies have shown that as the length of a spacer increases so does cellular transfection rates. However, as the length of the spacer group becomes too large cellular transfection will be reduced due to the instability of the structure (Wettig et al., 2007). It has been determined that the addition of an NH group within the spacer group will increase transfection rates. A study presented by Wettig and colleagues determined that gemini surfactants containing a spacer length of 7 with the addition of an NH group could bind the greatest amount of DNA and have the highest transfection efficiencies when compared to the other experimental groups (Figure 7) (Wettig, et al 2007).

A)



B)

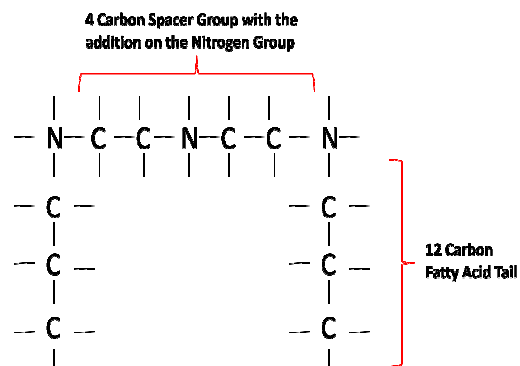


**Figure 7: Chemical Structure of Gemini Surfactants Exhibiting Different Spacer Groups:** A) Illustration of gemini surfactant 16-3-16 structure. The center spacer group is composed of three carbons linked together; B) illustrates the spacer structure of gemini surfactant 16-5NH-16, where there is an addition of a nitrogen group within the spacer.

### **3.4 Colloidal Stability Measured Through Zeta Potential**

When designing transfection reagents for gene carriers it is important to understand their interactions at the colloidal level. If a system is not stable at the particle level transfection rates will decrease. Particle size and charge play dual roles in the stability of a colloidal system.

Zeta potential can be defined as the overall charge a particle holds in solution. For a stable colloidal system to be achieved, zeta potentials must reach + or – 30 mV. This value indicates whether or not there is enough electrostatic repulsion between particles to create a stable particle system (Alatorre-Meda et al., 2010).

As particles acquire a more neutral charge in a system, they become more attracted to each other. This attraction of particles is known as flocculation. As particles begin to flocculate, they form large aggregates that begin to sediment out of the system. Colloidal stability in a particle system is of particular importance when developing lipid gene carriers for intravenous administration. Stable, highly charged small particles allows lung clearance during administration and prevents the of blockage of small arteries or veins which can cause ischemic tissue or even death while in circulation (Kirby et al, 2003; Zhdanov et al., 2002).

### **3.5 Cationic Lipids for Drug and Gene Delivery**

The general mechanism of transfection using non-viral vectors is achieved through endocytosis of a target cell (Kheirrolomoom, et al., 2007; Kirby et al., 2003). Compared to viral vectors, the delivery of genes and therapeutic agents using cationic lipids must overcome several cellular barriers to result in a successful transfection. A virus has evolved naturally over millions of years to associate with a cells surface and efficiently delivery its contents into a target cell with extreme success rates. Unfortunately, cationic lipids have not naturally evolved mechanisms to enter into a target cell and require different intercellular delivery pathways. For transfection to be

successful in a target cell, the efficiency of transfection is highly dependent upon the lipid structure, DNA packing and size (Ma, et al 2007; Zhdanov et al., 2002; Alatorre-Meda et al., 2010). The association of DNA to a cationic lipid is achieved through electrostatic forces (zeta potential). Once DNA has bound to the lipoplex it is crucial that the lipoplex still holds a positive charge since the cellular membrane charge of a target cell is negative (Ma, et al 2007).

Successful *in vivo* delivery of a lipoplex into a target tissue or cell occurs through several stages. First, selected DNA for delivery must be appropriately bound and protected by the gene delivery agent or lipoplex (Kirby et al., 2003; Zhdanov et al., 2002; Alatorre-Meda et al., 2010). Second, the cargo bound to the lipoplex must be transported to the target tissues through IP injection or intravenous administration while maintaining colloidal stability (Kirby et al., 2003). Third, bound cargo must enter the cell through endocytosis which occurs through electrostatic interactions. Fourth, bound cargo to lipoplex is internalized forming an endosome in the cell where DNA must dissociate from the lipoplex appropriately before becoming degraded by the lowering endosomal pH (Kirby et al., 2003; Hoekstra et al., 2007). It is at this stage of transfection the addition of an NH group in gemini surfactants spacer group results in higher transfection rates (Ma et al., 2008; Wettig, et al 2007; Kirby et al., 2003). The NH group present in the spacer group of a gemini surfactant is exceedingly sensitive to pH changes and allows DNA dissociation readily, compared to other gemini surfactant spacer groups (Wettig et al., 2007; Luciani et al., 2007). Fifth, the dissociated DNA must be transported to the nucleus and become expressed. All stages of transfection using non-viral vectors have several intracellular obstacles to overcome and expression can be extremely dependent on structure, size of particle, charge, and stability of the lipoplex during the different stages of transfection (Ma et al 2007; Kirby et al., 2003; Zhdanov et al., 2002). These obstacles/barriers of gene delivery using non-viral gene carriers, have resulted in the development of strategies to increase transfection, particularly for their *in vivo* use. A novel gene delivery system called ultrasound targeted microbubble destruction (UTMD) has been designed to help overcome these cellular barriers improving transfection rates *in vivo* (Unger et al., 2001).

### **3.6 Ultrasound Targeted Microbubble Destruction**

Ultrasound targeted microbubble destruction (UTMD) is a new gene delivery system developed to increase transfection rates of non-viral gene carriers for their *in vivo* use. UTMD has been designed to help overcome cellular barriers and the difficulties using non-viral vectors to improve successful plasmid DNA delivery. UTMD results in high organ specificity, low invasiveness and a decreased immune reaction using its cationic counterparts (Mayer et al., 2008; Christiansen et al., 2003; Davis et al., 2002). This system combines ultrasound and cationic lipid microbubbles for gene delivery (Unger et al., 2001; Ohlerth, et al., 2007; Mayer et al., 2008).

### **3.7 Microbubbles**

Microbubbles are small gas-filled colloidal particles composed of either monovalent cationic lipids or protein-polymers, and can range in size from 1-8 $\mu$ m, depending on the target tissue involved (Thatte et al., 2005; Tinkov et al., 2008; Sek-Wen Hui et al., 2008). The core of a microbubble is displaced using stable heavy gasses; this allows stability during circulation, contrast for visual ultrasound, and explosive drug/gene delivery properties. Microbubbles can be loaded with drugs or DNA in many different ways: attachment to the membrane using electrostatic interaction, encapsulation, the use of a ligand, or the incorporation using multilayer microbubbles (Dijkmans et al., 2004). Until the 1990's microbubbles were known as contrast agents and used for diagnostic purpose. Microbubble contrast agents were combined with ultrasound for right heart opacification and cardiac shunt diagnostics. When combined with low frequency ultrasound the gas filled core causes white reflections or contrast allowing their movement to be monitored while in circulation (Tinkov, et al. 2008; Linder et al., 2004; Yoon et al., 2010). However, the half life of diagnostic contrast agent microbubbles was limiting, only remaining stable in circulation for approximately five minutes, due to an unstable shell. Microbubble size limited their use to diagnostics and large organ perfusion. These microbubbles were known as first generation microbubbles (Tinkov, et al. 2008; Linder et al., 2004).

Second generation microbubbles were developed to overcome previous obstacles by increasing stability and reducing size, but a reduced half life was still limiting their use. Eventually, the core of second generation microbubbles, which consisted of room air, was replaced with a stable gas such as perfluorocarbons. Using a stable gas such as perfluorocarbons prolongs stability in circulation for greater than 15 minutes (Tinkov, et al., 2008; Mayer, et al., 2008). These non-viral stable colloidal particles are now being explored to be used as vehicles to deliver drugs or genes into a target tissue or cell in combination with high frequency ultrasound.

### **3.8 UTMD Delivery Mechanism**

It is the incorporation of both ultrasound and microbubbles which make the UTMD system unique. High frequency ultrasound is used to destroy the gas-filled microbubbles, this not only guarantees the release of the cargo in the vicinity of the target cells, but also facilitates cargo uptake through the production of microjets from the exploding microbubbles (Pitt et al., 2004; Dijkmans et al., 2004; Unger et al., 2001; Meijering et al., 2009; Chen et al., 2006). When exposed to high frequency ultrasound, the gas present within the core of the microbubble to become highly compressed; this compression causes the microbubble to explode, releasing its contents at the target tissue. This mechanism of action is also known as cavitation (Figure 8) (Pitt et al., 2004). The collapse of the microbubbles from high frequency ultrasound creates high-energy microstreams or microjets. These microjets cause stress to the surrounding cells, increasing their cellular membrane permeability (Unger et al., 2001; Dijkmans et al., 2004; Bekeradjian et al., 2007; Borden et al., 2005).



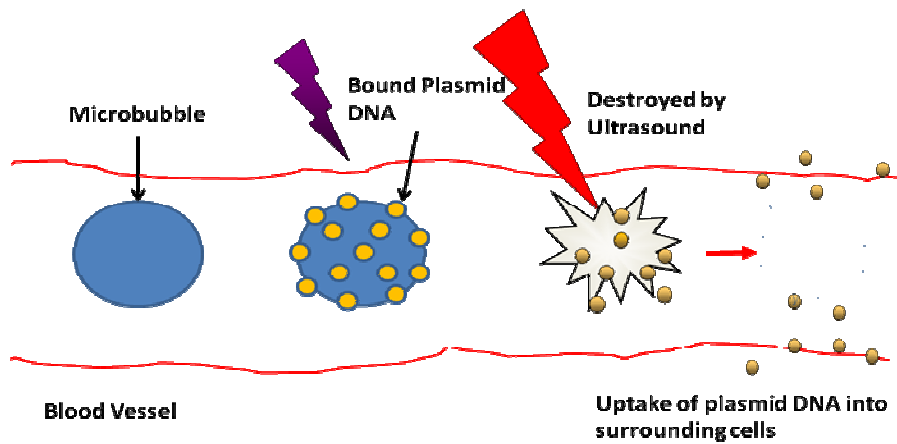


**Figure 8: Ultrasound Targeted Microbubble Destruction:** This figure illustrates the action of ultrasound targeted microbubble destruction. Microbubbles attached with drugs or genes are perfused through the circulation, targeted using ultrasound and destroyed with high frequency ultrasound. The result is the uptake of the drugs or gene by the surrounding cells.

The exact mechanism of cellular uptake of therapeutic agents into a cells' cytosol using UTMD is not completely understood (Meijering et al., 2009). It has been recently suggested that one mechanism of cellular uptake using UTMD is induced by transient holes, or pores in the cellular membrane. In contrast, it is proposed that ultrasound causes small depressions rather than pores in the cellular membrane which induces endocytosis (Meijering et al., 2009; Chen et al., 2006).

Several research groups have tried to investigate the exact mechanism of UTMD and how its action results in cellular transfection. Studies by Meijering and colleagues (2009) reported that cell cultures exposed to ultrasound causes pore formation in the plasma membrane. These pores result in the influx of  $\text{Ca}^{2+}$  inside the cell. This rise in calcium concentrations inside the cell results in the increased formation of hydrogen peroxide within the cells cytosol. This observation was also reported by the Jufferman's group, where a significant increase in cytosolic hydrogen peroxide was observed after cells were exposed to ultrasound (Juffermans et al., 2006). This increase in hydrogen peroxide was associated with the influx of  $\text{Ca}^{2+}$  inside the cell due to cellular membrane permeability. The increase in hydrogen peroxide has a direct correlation to endocytosis (Meijering et al 2009).

Endocytosis into a cell can occur through several different endocytotic pathways: clathrin-mediated endocytosis, caveolin-mediated endocytosis and macropinocytosis (Meijering et al., 2009). After the confirmation that ultrasound results in a  $\text{Ca}^{2+}$  influx into the cell, the Meijering group further investigated the process of endocytosis with UTMD by using individual blockers of the three main pathways of endocytosis. This research group was able to conclude that endocytosis and pore formation to deliver therapeutic compounds is dependent on molecular size of the drug/gene delivery agent (Meijering et al 2009). When all endocytotic pathways were blocked, the uptake of therapeutic agents was restricted, but only to molecules with a size greater than 500kDa. These results supported but did not completely explain the processes of UTMD during cell mediated uptake of therapeutic agents. Both endocytosis and pore formation seem to

play a dual role but the complete mechanism of this uptake is still not completely understood (Meijering et al 2009).

### **3.9 UTMD and its *In Vivo* Application**

Several scientists have been successful in delivering genes into target tissues using monovalent constructed microbubbles with the UTMD system. Work presented by Shuyuan Chen has illustrated the success in using monovalent Lipofectamine 2000 microbubbles and UTMD in delivering a target gene into rat pancreatic islets. These scientists were successful in the targeting of a reporter gene into pancreatic islets by using the rat insulin 1 promoter (RIP) and successfully delivering a  $\beta$ -cell specific hexokinase I gene to increase insulin secretion using Lipofectamine 2000 microbubbles (Chen et al., 2006). The scientists concluded that the use of monovalent Lipofectamine 2000 microbubbles with high frequency ultrasound resulted in the delivery of DNA with limited inflammatory response. Monovalent microbubbles loaded with plasmid DNA can be delivered into the circulation reducing invasive surgery, high organ specificity (with the use of ultrasound) resulting in no damage to pancreatic islets after microbubble infusion with ultrasound (Chen et al., 2006). Work presented by Bekeredjian, confirmed gene delivery of CMV-luciferase plasmids to the heart, achieving high transgene expression and high organ specificity four days after exposure also with the use of monovalent microbubbles (Bekeredjian et al., 2003). A third study presented by Bekeredjian also illustrated the successful use of UTMD in delivering plasmid DNA to the skeletal muscle of rats. High gene expression was shown seven days after administration of UTMD with the VEGF (vascular endothelial growth factor) gene. This study demonstrated that ultrasound combined with monovalent microbubbles is a safe delivery system to muscle tissue and will result in high gene expression (Bekeredjian et al., 2003)

### **3.10 UTMD as a tool for diabetes treatment**

UTMD-based gene delivery holds great promise for gene therapy as this method has overcome the difficulties and barriers that impeded the existing viral vector-based methods for successful clinical application (Unger et al., 2001; Bekeredjian et al., 2003; Yoon et al., 2010). UTMD has proven to be less immunogenic, less cytotoxic and more target specific than the viral vector based methods (Mayer et al., 2008; Bekeredjian et al., 2003). The target specificity of UTMD can even be increased by placing the gene of interest under a cell type-specific promoter, restricting its expression to certain cells in the targeted organ (Chen et al., 2006; Christiansen et al., 2003).

The identification of genes involved in  $\beta$ -cell function, survival, growth and neogenesis, suggests that UTMD holds great potential in the treatment of diabetes as the restoration of  $\beta$ -cell mass and/or improvement of  $\beta$ -cell function would alleviate the metabolic burden in both type 1, MODY and type 2 diabetics (Stock et al., 2004).

Recent work published by Dr. P.A. Grayburn focused on delivering the vascular endothelial growth factor (VEGF) gene to the liver using monovalent microbubbles incorporated with UTMD to promote islet revascularization post transplantation. Remarkably, the results demonstrated an increase in both vessel growth and density in transplanted islets, drastically improving their functionality post transplantation (Shimoda et al., 2010). A second study by Dr. P.A. Grayburn demonstrated the successes of monovalent microbubbles with the UTMD technique by delivering a series of genes to stimulate endocrine development. Six genes such as Pax4, NKx2.2, NKx6.1, Ngn3, Pdx and Mafa, were delivered into streptozotocin-induced diabetic rats and resulted in islet regeneration and restoration of both  $\beta$ -cell mass and normalized of blood glucose levels in the animal models (Chen et al., 2010).

As clearly demonstrated, UTMD as a gene delivery system to treat disease, such as diabetes has considerable potential. Previous work has demonstrated and supported its success using monovalent cationic lipid microbubbles when corporate with UTMD. However, monovalent

cationic lipid microbubbles such as Lipofectamine 2000 are very expensive to produce, and the quantities required to bind sufficient amounts of DNA is quite high; limiting their clinical application. Gemini surfactants have been recognized for their increased DNA binding capabilities and transfection rates equal to monovalent lipids but for a fraction of the cost (Wettig, et al., 2007; Kirby et al., 2003). Developing a cost efficient microbubble gene carrier to incorporate with ultrasound while acquiring equal transfection rates to monovalent microbubble, would increase UTMD's clinical application for gene therapy for diabetes.

### *Purpose*

The purpose of this study is to develop an optimized microbubble gene carrier using a new family of cationic lipids known as gemini surfactants to incorporate with ultrasound, and compare transfection capabilities *in vitro* to commercially used monovalent cationic lipid microbubbles using the UTMD gene delivery technique. The major objectives and aims are:

### *Objective 1: Optimization of a Microbubble Gene Carrier*

#### *Aim 1:*

Assess size and charge of gemini surfactants 16-3-16 and 16-7NH-16 and compare to Lipofectamine 2000

Hypothesis (1): Gemini surfactants would achieve a smaller particle size with increased charge based on the additional spacer group.

#### *Aim 2:*

Assess the effects of DNA binding on particle size and charge of gemini surfactants 16-3-16 and 16-7NH-16

Hypothesis (2): A reduced particle size and reduced loss in surface charge would be achieved from gemini surfactant 16-7NH-16 after the addition of DNA due to the N-H *imino* group present within the spacer.

Objective 2: In Vitro Assessment of Optimized Microbubble Gene Carrier

*Aim 4: Human Embryonic Kidney Cells – HEK 293 and Rat Insulinoma Cells – INS-1 832/13*

Assess transfection efficiencies and toxicity effects of gemini surfactant microbubbles *in vitro* using HEK 293 and INS-1 832/13 cells. Compare transfection capabilities to monovalent cationic lipids

Hypothesis (3): Gemini surfactant 16-7NH-16 microbubbles would exhibit higher transfection rates with reduced toxicity based on the increased DNA binding effects demonstrated by the N-H *imino* group reducing the amount of compound required for transfection, while maintaining a reduced particle size and increased surface charge.

Objective 3: Assess UTMD DNA release

(1) Assess pAMAXA plasmid GFP DNA binding and release using ultrasound on gemini surfactant microbubbles

Hypothesis (4): Ultrasound exposure to gemini surfactant 16-7NH-16 microbubbles would release DNA cargo based on the explosion properties ultrasound exposure has on compressed perfluorobaron gas.

# Chapter 4

## 4.1 Methods

### *Materials*

Gemini surfactants 16-3-16 and 16-7NH-16 were synthesized and provided by Dr. Shawn Wettig from the University Of Waterloo School Of Pharmacy. Monovalent cationic lipids Lipofectamine 2000, Fugene, DOTAP and neutral lipids DL- $\alpha$ -Phosphitdylcholine, Dipalmitoyl (DPPC) and L- $\alpha$ -Phosphatidylethanolamine, dioleoly were purchased from Sigma. Plasmid Endofree Plasmid Giga kit was purchased from QIAGEN. Visual Sonics SoniGene 1 MHz probe, Visual Sonics Vevo System and wavelength clear ultrasound gel was purchased from visual sonics. The SoniGene 1MHz probe applies 1MHz of ultrasound to causes sonoporation and microbubble destruction to target cells at intensities that can range between 0.5 and 2.0 W/cm<sup>2</sup>. The Visual Sonics Vevo system is used to identify the region of interest and allow image-guided injection of microbubble gene carriers.

### *Plasmid DNA Synthesis*

Plasmid pAMAXA GFP DNA plasmid was used that had a CMV driven promoter to express GFP. Plasmid DNA was propagated from *Escherichia coli* and purified using a QIAGEN EndoFree Plasmid Giga kit (12391) following the protocol provided by the manufacturer.

### *Synthesis of Cationic Lipid Stocks*

Lipid stocks were prepared similar to the protocol developed by Chen (2007). 25 mg of neutral lipids DL- $\alpha$ -Phosphitdylcholine, Dipalmitoyl (DPPC) (Sigma P-5911), 2.5 mg of L- $\alpha$ -Phosphatidylethanolamine, dioleoly (DOPE) (Sigma P-1223) and 13.5 mg of gemini surfactant

was added to 1 mL of modified PBS (Hyclone), achieving a 2:1 molar ratio (neutral lipids to gemini surfactant). Lipid stock solutions were sonicated (Probe Sonicator Misonix Ultrasonic Liquid Processor XL-2000) for approximately 30 seconds at an output of 3 watts.

#### *Synthesis of Microbubbles*

Microbubble lipid solution was prepared as previously described (Chen 2007) by measuring out 10  $\mu$ l of glycerol (Sigma), 880  $\mu$ l modified PBS, 60  $\mu$ l Opti-MEM and 50  $\mu$ l of premade lipid stock (see above). Microbubble lipid solutions were perfused with perfluorocarbon gas and vortexed for approximately 30 seconds.

#### *Displacement of the Aqueous Center*

Using a needle, neutral microbubble lipid solution was injected into clear wavelength ultrasound gel. Visual Sonics Vevo system was used to visually confirm the displacement of the aqueous center by identifying white contrast in ultrasound gel; and a SoniGene 1 MHz probe was applied for microbubble destruction at 1.0 W/cm<sup>2</sup>.

#### *Particle Size and Charge*

Microbubble lipid solution was used to measure microbubble size and charge. Microbubble particle size was measured in  $\mu$ m using dynamic light scattering on the Zetasizer (Nano ZS, Malvern). Microbubble particle charge was determined through electrophoresis and measured in mV by the Zetasizer (Nano ZS, Malvern), the same microbubble lipid solution was used to measure both particle size and charge.



### *Gemini Surfactant pAMAXA Plasmid DNA Binding Analysis through Electrophoresis gel*

Neutral lipid and gemini surfactant 16-7NH-16 2:1 ratio microbubbles were prepared with the addition of 25 µg of plasmid pAMAXA GFP DNA. Microbubbles and pAMAXA plasmid DNA were loaded onto a 1% agarose gel.

### *In Vitro Assessment of Optimized Microbubbles using UTMD*

HEK 293 cells and INS-1 832/13 were cultured in RPMI 1640 medium containing 10 % fetal calf serum, 10 mmol/l HEPES, 2 mmol/l L-glutamine, 1mmol/l Na-pyruvate, 50 µmol/l-mercaptoethanol, 100 U/ml of penicillin, and 100 µg/ml streptomycin (Sigma) at 37 °C and 5% CO<sub>2</sub>. Both cell lines were added to a 12 well plate at densities of 0.75 x10<sup>6</sup> cells per well. Cells were left to adhere to culture plate 24 hours or kept in suspension. Four microbubble solutions were tested in cell culture using ultrasound 1) Lipofectamine 2000, following manufactures protocol, 2) Fugene, following manufactures protocol 3) DOTAP, following manufactures protocol 4) Gemini surfactant 16-7NH-16. 25 µg of plasmid pAMAXA GFP DNA was additionally added to all microbubble solutions. SoniGene 1 MHz ultrasound probe was used and exposed to cells at intensities of 1.0 W/cm<sup>2</sup>, 1.5 W/cm<sup>2</sup> and 2.0 W/cm<sup>2</sup>. Cellular transfection rates were determined though visual estimation of the percentage of cells expressing GFP using fluorescent microscopy. Cell viability was assessed by the number of cells not adhered to culture plate after transfection, this determined the death rate after transfection.

### *Plasmid DNA Binding and Release using UTMD*

Neutral and gemini surfactant 16-7NH-16 microbubbles 2:1 and 10:1 ratio were prepared with the addition of 50 µg of plasmid pAMAXA GFP DNA. A SoniGene 1 MHz probe was is applied to samples and loaded on a 1 % agarose gel.

# Chapter 5

## 5.1 Results

### Overview:

The research in this study focused on developing a gemini surfactant microbubble capable of gene delivery into HEK 293 and INS-1/13 cells using high frequency ultrasound. This was achieved through detailed investigation of two cationic gemini surfactants 16-3-16 and 16-7NH-16 as possible microbubble gene carriers. These surfactants microbubbles were compared to commercially used monovalent microbubbles Lipofectamine 2000, Fugene and DOTAP for transfection capabilities. Particle size, zeta potential, colloidal stability and DNA binding was heavily assessed.

## 5.2 Optimization of a Microbubble Gene Carrier

### *Assessing Gemini Surfactant Particle Size*

Assessing gemini surfactant particle size and comparing to monovalent Lipofectamine 2000 would give a good indication as to whether these surfactants would be suited for gene delivery *in vivo* for intravenous administration and cellular uptake. It was hypothesized that both gemini surfactant microbubbles would achieve a smaller particle size based on the addition of the spacer group. Particle size of cationic microbubbles containing gemini surfactants 16-3-16, 16-7NH-16, and Lipofectamine 2000 was investigated using dynamic light scattering and compared to neutral lipid microbubbles (negative control). Figure 9 illustrates microbubble particle size among each group. Smallest microbubble particle size was achieved from both gemini surfactant 16-3-16 at 0.167  $\mu\text{m}$  and 16-7NH-16 at 0.275  $\mu\text{m}$  when compared to Lipofectamine 2000 at 3.09  $\mu\text{m}$  and neutral lipid MB at 1.54  $\mu\text{m}$ .

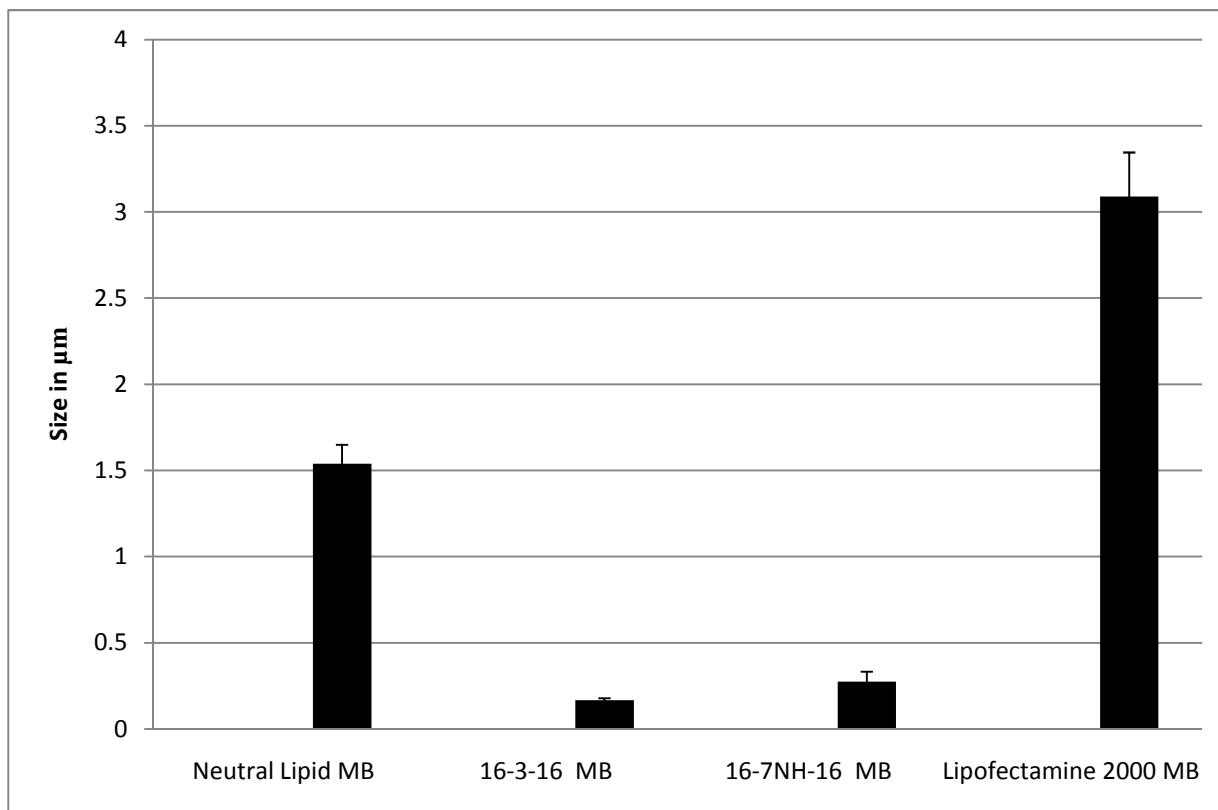


**Figure 9: Particle size comparison of cationic gemini surfactants 16-3-16, 16-7NH-16, and Lipofectamine 2000 Microbubbles:** Three experimental groups were compared to control microbubbles (neutral lipid MB, made with DPPC and DOPE). 1) Gemini surfactant 16-3-16 at a 2:1 ratio of neutral lipids (DPPC and DOPE) to surfactant MB, 2) Gemini surfactant 16-7NH-16 at a 2:1 ratio of neutral lipids (DPPC and DOPE) to surfactant MB, 3) Lipofectamine 2000 MB. Particle size was measured using the dynamic light scattering on a Malvern Zetasizer Nano ZS. The error bars represent the difference between particle size measurements,  $n=1$  and measurements were taken three times at the particles surface using dynamic light scattering. Smallest particle size was achieved by both gemini surfactants 16-3-16 at  $0.167 \mu\text{m}$  and 16-7NH-16 at  $0.275 \mu\text{m}$  when compared to Lipofectamine 2000 ( $3.09 \mu\text{m}$ ) and neutral lipid microbubbles ( $1.54 \mu\text{m}$ )

### *Particle Surface Charge Analysis through Zeta Potential*

Particle surface charge was compared to Lipofectamine 2000. Determining a particles surface charge confirms not only colloidal stability but also DNA binding potential. Particle charge was determined though electrophoresis using a Zetasizer (Malvern Nano ZS). Figure 10 illustrates the zeta potential achieved from microbubble gemini surfactants 16-3-16, 16-7NH-16, Lipofectamine 2000 MB and compared to neutral lipid microbubbles (negative control). Gemini surfactant microbubble particle charge was the highest detected among each group measuring  $+29$  mV for surfactant 16-3-16 and  $+30$  for surfactant 16-7NH-16. The zeta potential detected by both gemini surfactant microbubbles exhibited little difference, with an average surface charge of approximately  $+30$  mV. Lipofectamine 2000 MB measured  $-6.2$  mV and  $+9.8$  mV for neutral lipid MB resulting in the lowest charge, indicating an unstable particle system.

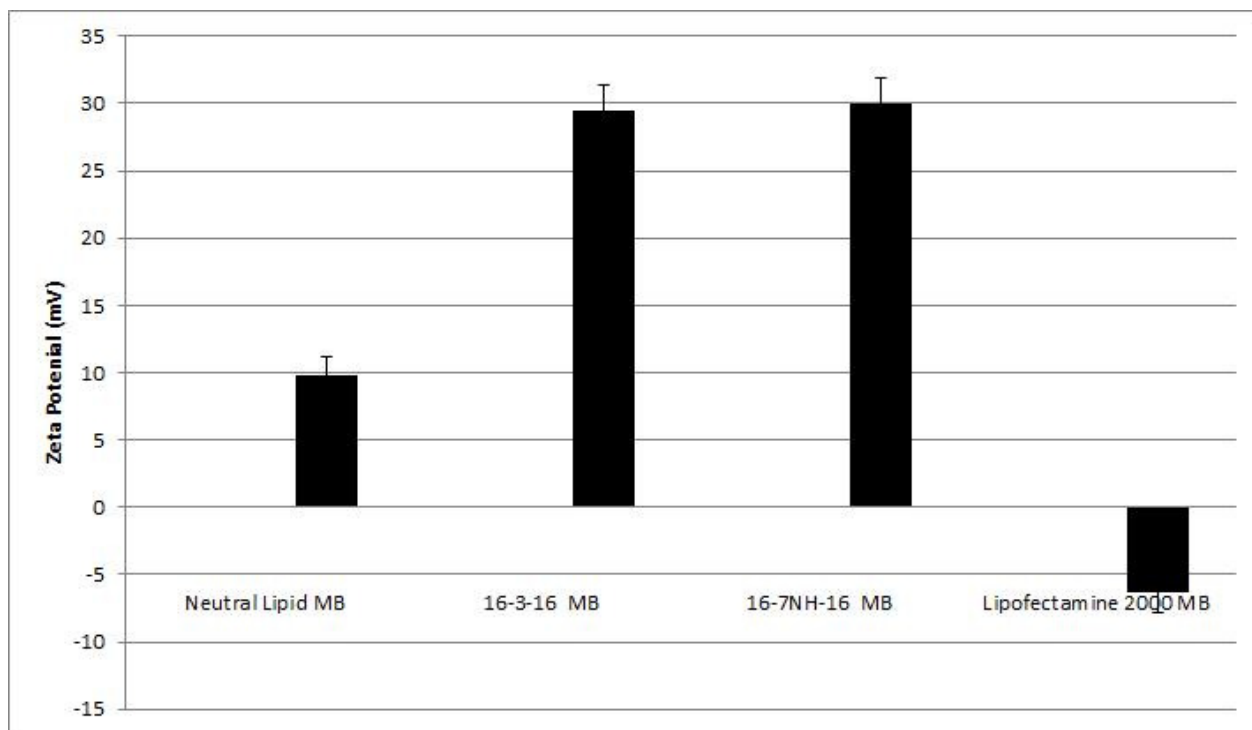


**Figure 10: Zeta potential comparison of cationic gemini surfactants 16-3-16, 16-7NH-16, and Lipofectamine 2000 Microbubbles:** Three experimental groups were compared to control microbubbles (neutral lipid MB, made with DPPC and DOPE). 1) Gemini surfactant 16-3-16 at a 2:1 ratio of neutral lipids (DPPC and DOPE) to surfactant MB, 2) Gemini surfactant 16-7NH-16 at a 2:1 ratio of neutral lipids (DPPC and DOPE) to surfactant MB, and 3) Lipofectamine 2000 MB. Zeta potential is determined by electrophoresis on the Malvern Zetasizer Nano ZS and is measured in mV. Measurements were taken at the particles surface and a charge determined. The error bars represent the difference between charge measurements, n=1 and measurements were taken three times using electrophoresis. Gemini surfactant 16-3-16 measured a surface charge of +29 mV and 16-7NH-16 +30 mV indicating a stable colloidal system when compared to Lipofectamine 2000 MB measuring -6.2 and neutral lipids DPPC and DOPE MB at +9.8 mV.

*Plasmid pAMAXA GFP DNA binding effects on particle size*

Determining DNA binding and its effects on particle size of non-viral gene carriers is a critical phase to investigate, considering *in vivo* application. Figure 12 represents the results of the addition of 50 µg of plasmid pAMAXA GFP DNA and the effects on microbubble particle size. The results indicate the addition of plasmid pAMAXA GFP DNA increases microbubble particle size. Gemini surfactant 16-3-16 particle size increased from 0.167 µm to 2.23 µm after the addition of pAMAXA GFP DNA. Gemini surfactant 16-7NH-16 increased in particle size from 0.275 µm to 0.74 µm after the addition of pAMAXA GFP DNA. Gemini surfactant microbubbles 16-3-16 exhibited the largest increase in particle size when compared to surfactant 16-7NH-16 microbubbles demonstrate gemini surfactant 16-7NH-16 superior binding and DNA compacting properties.

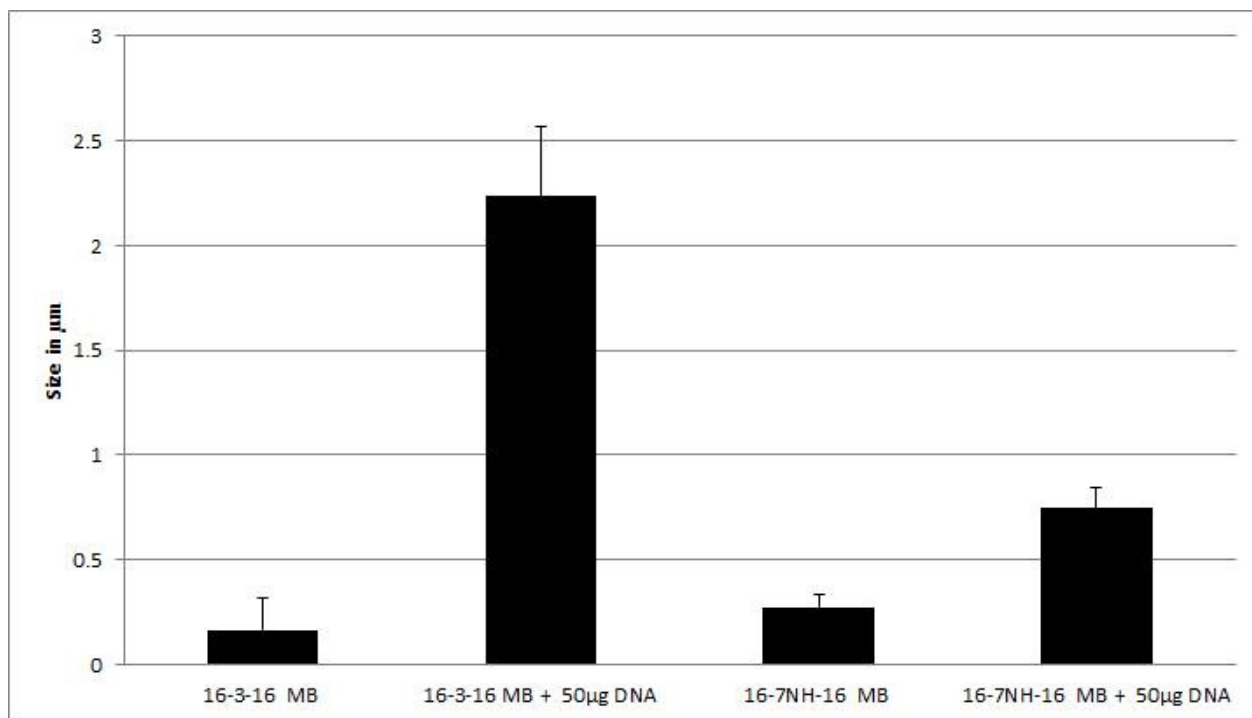


**Figure 11: Particle size comparison of cationic gemini surfactants with and without the addition of plasmid pAMAXA GFP DNA:** Graph illustrating the average particle size of gemini surfactants 16-3-16 and 16-7NH-16 MB with and without the addition of plasmid pAMAXA GFP DNA. Two experimental groups were examined 1) Gemini surfactant 16-3-16 at a 2:1 ratio of neutral lipids (DPPC and DOPE) to surfactant with and without the addition of 50 µg of DNA, 2) Gemini surfactant 16-7NH-16 at a 2:1 ratio of neutral lipids (DPPC and DOPE) to surfactant MB with and without the addition of 50 µg of DNA. Particle size increases with the addition of 50 µg of plasmid pAMAXA GFP DNA in both surfactants. Particle size was measured using the dynamic light scattering on a Malvern Zetasizer Nano ZS. The error bars represent the difference between particle size measurements, n=1 and measurements were taken three times at the particles surface using dynamic light scattering. Smallest particle size with the addition of 50 µg of DNA was achieved by gemini surfactant 16-7NH-16 increasing from 0.275 µm to 0.74 µm when compared to gemini surfactant 16-3-16 increasing from 0.167 µm to 2.23 µm.

*Plasmid pAMAXA GFP DNA binding effects on zeta potential*

The stability of a colloidal system can be changed or become lost with the addition of other cations or anions. Figure 13 illustrates the effect 50  $\mu\text{g}$  of plasmid pAMAXA GFP DNA had on zeta potential of both gemini surfactant microbubbles. The addition of pAMAXA plasmid GFP DNA increased the zeta potential of both gemini surfactant microbubbles. Gemini surfactant 16-3-16 increased in surface charge from  $+34$  mV to  $+39$  mV after the addition of pAMAXA GFP DNA, and surfactant 16-7NH-16 increased from  $+34.6$  mV to  $+37.74$  mV after the addition of pAMAXA GFP DNA. These results demonstrate the direct influence the addition of DNA has on particles charge ultimately changing the properties of a colloidal particle system.



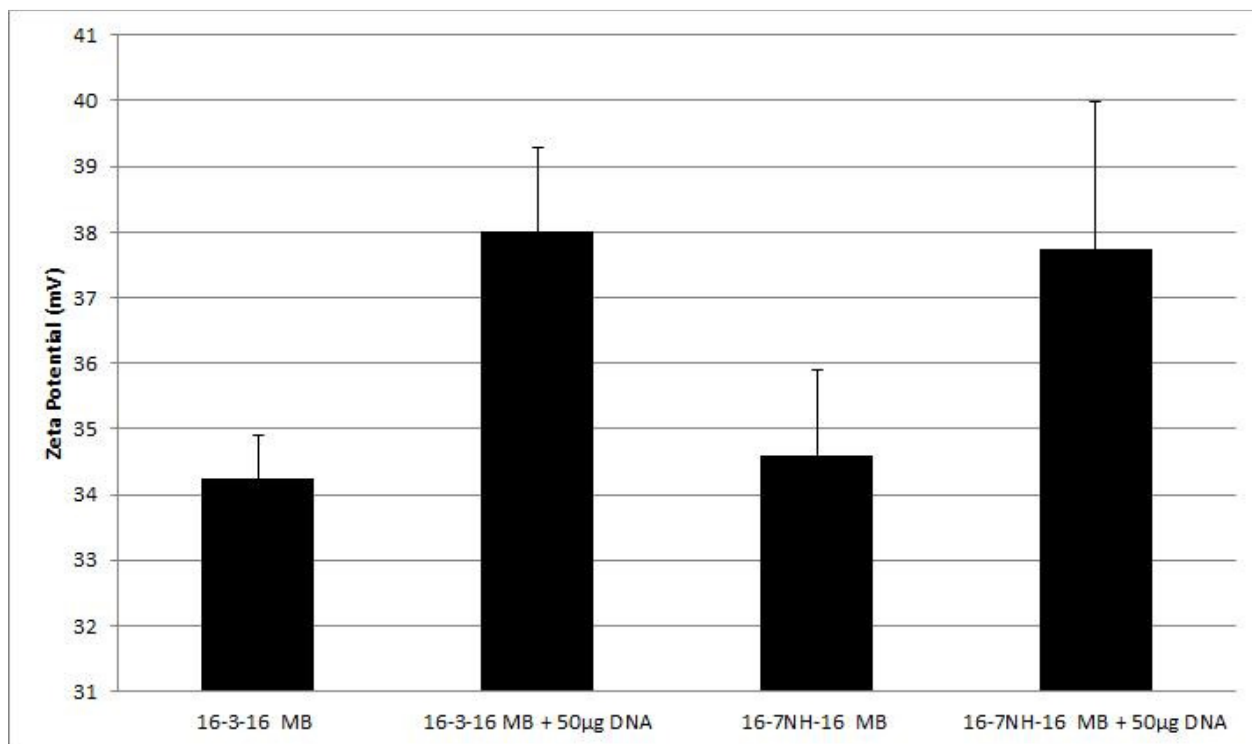


**Figure 12: Zeta potential comparison of gemini surfactants 16-3-16 and 16-7NH-16 with and without the addition of plasmid pAMAXA GFP DNA:** Graph illustrating the average zeta potential achieved by experimental groups 1) Gemini surfactant 16-3-16 at a 2:1 ratio of neutral lipids (DPPC and DOPE) to surfactant with and without the addition of 50 µg of DNA, 2) Gemini surfactant 16-7NH-16 at a 2:1 ratio of neutral lipids (DPPC and DOPE) to surfactant MB with and without the addition of 50 µg of DNA. Zeta potential is determined by electrophoresis on the Zetasizer (Malvern Nano ZS) and is measured in mV. Measurements were taken at the particles surface and a charge determined. The error bars represent the difference between charge measurements, n=1 and measurements were taken three times using electrophoresis. Particle charge increases with the addition of 50 µg of plasmid pAMAXA GFP DNA. Gemini surfactant 16-3-16 increased in surface charge from +34 mV to +39 mV and gemini surfactant 16-7NH-16 from +34.6 mV to +37.74 mV after the addition of pAMAXA GFP DNA.

*Plasmid pAMAXA GFP DNA binding analysis of gemini surfactant 16-7NH-16 through gel electrophoresis*

Determining DNA binding and condensing properties of a non-viral gene carrier gives insight into maximum binding potential and confirms DNA interaction. Gemini surfactant 16-7NH-16 was chosen for further investigation through gel electrophoresis due to higher DNA condensing properties (Wettig, et al., 2007). Figure 14 illustrates the binding capabilities of gemini surfactant 16-7NH-16 microbubbles with the addition of 25 µg of plasmid pAMAXA GFP DNA using gel electrophoresis analysis. Gemini surfactant 16-7NH-16 MB was compared to pure 25 µg plasmid pAMAXA GFP DNA and neutral lipid microbubbles with the addition of 25 µg of plasmid pAMAXA GFP DNA as controls. A DNA incubation time line was performed to determine if an incubation period is required to bind plasmid pAMAXA GFP DNA to gemini surfactant 16-7NH-16. The results confirm no pre-incubation period is required to fully bind and condense 25 µg plasmid pAMAXA GFP DNA to gemini surfactant 16-7NH-16 microbubbles. This interaction appears to occur rapidly once DNA is added to the lipid solution.

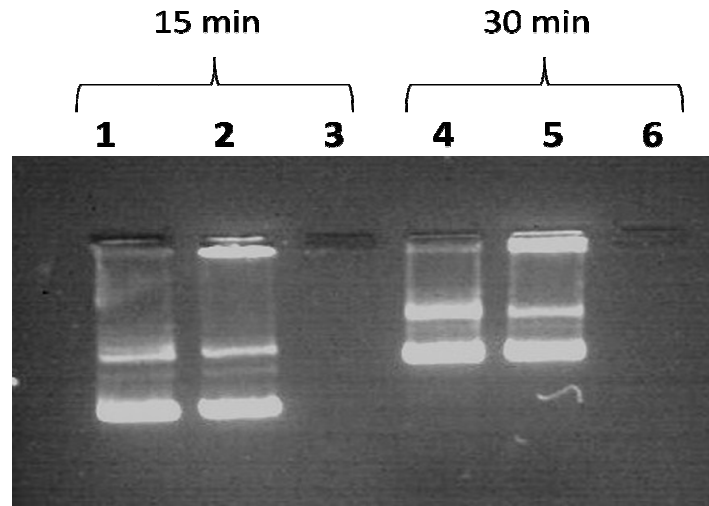


**Figure 13: Gemini surfactant plasmid DNA binding analysis through gel electrophoresis:** Gel electrophoresis image illustrating plasmid pAMAXA GFP DNA binding of gemini surfactant 16-7NH-16 MB. A time line of 15 and 30 minutes of incubation with plasmid pAMAXA GFP DNA was examined. Lanes 1, 2 and 3 were incubated with plasmid pAMAXA GFP DNA for 15 minutes. Lanes 4, 5 and 6 were incubated with pAMAXA GFP DNA for 30 minutes. Lane 1) 25  $\mu$ g plasmid pAMAXA GFP DNA (positive control), Lane 2) Neutrally charged lipid MB (DPPC and DOPE) + 25  $\mu$ g plasmid pAMAXA GFP DNA (negative control), Lane 3) Gemini surfactant 16-7NH-16 at a 2:1 ratio of neutral lipids (DPPC and DOPE) to surfactant MB + 25  $\mu$ g of plasmid pAMAXA GFP DNA. Lane 4) 25  $\mu$ g plasmid pAMAXA GFP DNA, Lane 5) Neutrally charged lipid MB (DPPC and DOPE), Lane 6) Gemini surfactant 16-7NH-16 at a 2:1 ratio of neutral lipids (DPPC and DOPE) to surfactant MB + 25  $\mu$ g of plasmid pAMAXA GFP DNA.

### 5.3 In Vitro Assessment of Optimized Microbubble Gene Carrier

#### *Assessing ultrasound transfection capabilities in attached HEK 293 cells*

Investigating and optimizing ultrasound transfection capabilities *in vitro* not only confirm the efficiency of ultrasound as a gene delivery system, but also provide useful information to test once this gene delivery system in an *in vivo* model. Figure 16 represents the results of the investigation; assessing ultrasound effects on cellular transfection in attached HEK 293 cells with gemini surfactant 16-7NH-16 microbubbles. Gemini surfactant microbubbles were synthesized and compared to controls, 1) Neutrally charged MB + 25  $\mu$ g plasmid pAMAXA GFP DNA (negative control), 2) Monovalent cationic lipid Fugene + 25  $\mu$ g plasmid pAMAXA GFP DNA (positive control), and 4) 25  $\mu$ g plasmid pAMAXA GFP DNA (negative control). After 48 hours cells were accessed for GFP expression. Cellular transfection rates were determined by visually estimating the percentage of cells expressing GFP using fluorescent microscopy after exposure to ultrasound (see figure legend for details). Positive control group Fugene + 25  $\mu$ g of plasmid pAMAXA GFP DNA demonstrated positive expression of GFP with transfection rates at 100 %. Negative control group neutrally charged MB exhibited a 15 % transfection rate, followed by a 15 % transfection rate from negative control 25  $\mu$ g plasmid pAMAXA GFP DNA at ultrasound intensity 2.0 W/cm<sup>2</sup>. Gemini surfactant 16-7NH-16 MB established a zero percent transfection rate at all ultrasound intensities investigated and 1 % transfection from control.

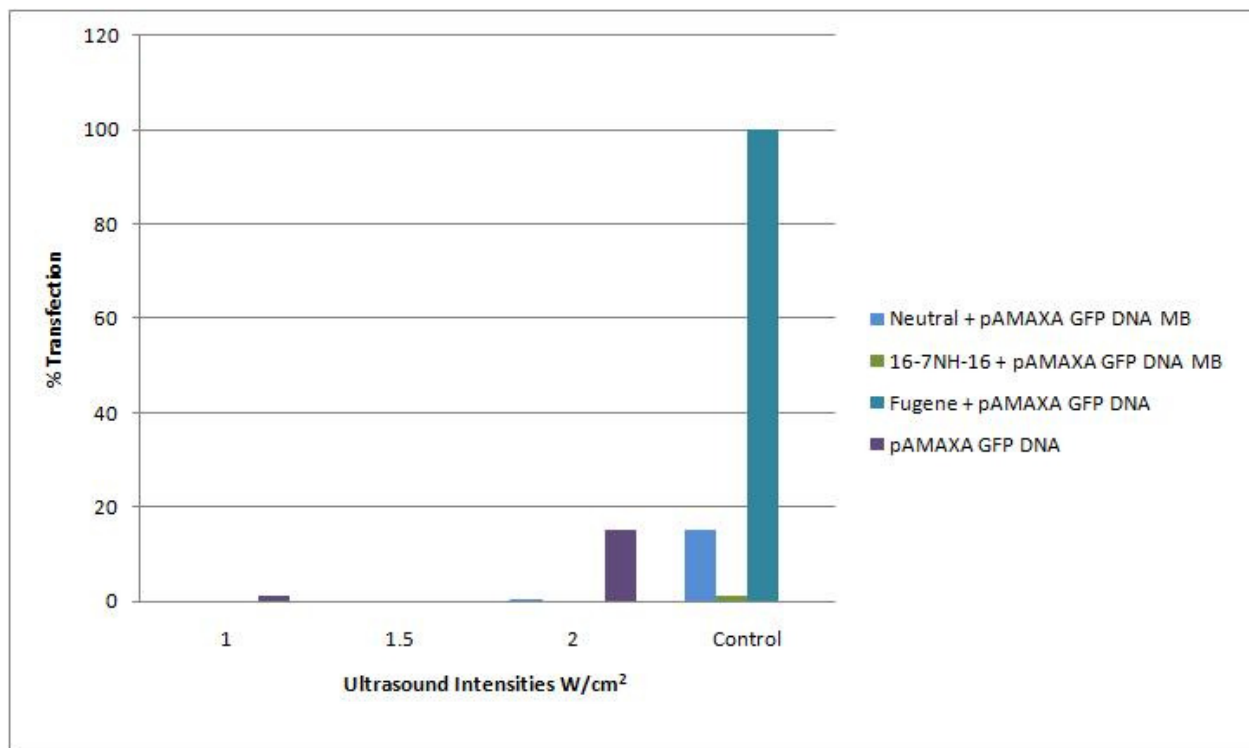


**Figure 14: Transfection efficiency comparison of pAMAXA plasmid GFP in attached HEK 293 cells using ultrasound:** After 48 hours of incubation, cells were assessed for GFP expression. Positive control Fugene + 25  $\mu\text{g}$  of plasmid pAMAXA GFP DNA, negative control neutral lipid microbubbles 10:1 ratio (DPPC:DOPE) + 25  $\mu\text{g}$  of plasmid pAMAXA GFP DNA and 25  $\mu\text{g}$  plasmid pAMAXA GFP DNA were compared to experimental group gemini surfactant 16-7NH-16 2:1 ratio (DPPC:DOPE:16-7NH-16) + 25  $\mu\text{g}$  of plasmid pAMAXA GFP DNA.  $n = 3$  for each group. Using a SoniGene 1 MHz probe, microbubbles were destroyed in cell culture solution. Ultrasound intensities investigated were 1.0  $\text{W}/\text{cm}^2$ , 1.5  $\text{W}/\text{cm}^2$ , and 2.0  $\text{W}/\text{cm}^2$

*Assessing ultrasound cell viability after transfection in attached HEK 293 cells*

Figure 17 illustrates the estimated percent cell viability in transfected HEK 293 cells using ultrasound. After 48 hours cells were assessed for viability. These results indicate gemini surfactant 16-7NH-16 MB + 25  $\mu$ g plasmid pAMAXA GFP DNA with the incorporation of the ultrasound technique results in high cell death rates. The most prevalent percent cell death rate was achieved from gemini surfactant 16-7NH-16 MB + 25  $\mu$ g plasmid pAMAXA GFP DNA at a ultrasound intensity 1.0 W/cm<sup>2</sup>, reaching death rates of 90 %. As ultrasound intensities decreased, gemini surfactant 16-7NH-16 MB demonstrated a drop in percent cellular death to approximately 45 % and maintained equal cell death rates between intensities 1.5 W/cm<sup>2</sup>, 2.0 W/cm<sup>2</sup> and including control. Cell death rate, on average, was low for both negative control group's neutrally charged MB + 25  $\mu$ g plasmid pAMAXA GFP DNA and 25  $\mu$ g plasmid pAMAXA GFP DNA with cell death rates less than 5 %. Zero percent cell death was observed from Fugene + 25  $\mu$ g plasmid pAMAXA GFP DNA (positive control).

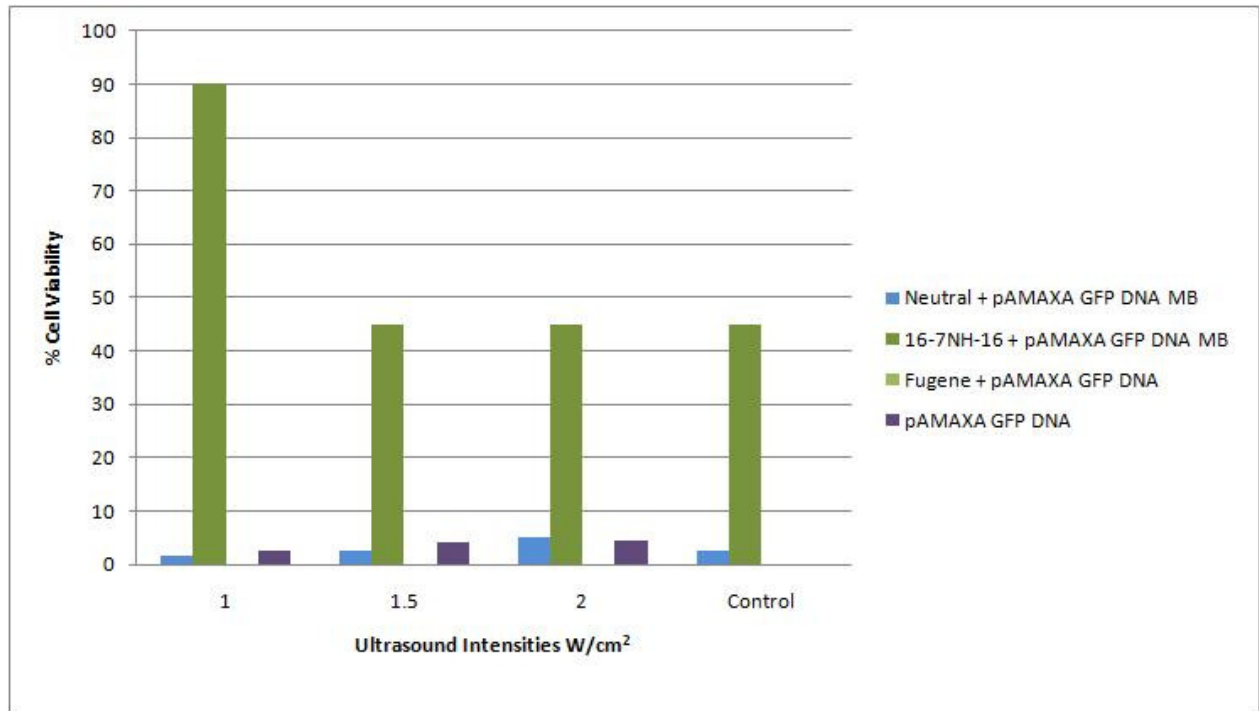


**Figure 15: Cell viability of transfected HEK 293 cells using ultrasound:** After 48 hours cell viability was assessed. Positive control Fugene + 25  $\mu\text{g}$  of plasmid pAMAXA GFP DNA, Negative control neutral lipid microbubbles 10:1 ratio (DPPC:DOPE) + 25  $\mu\text{g}$  of plasmid pAMAXA GFP DNA and 25  $\mu\text{g}$  plasmid pAMAXA GFP DNA were compared to experimental group tested gemini surfactant 16-7NH-16 2:1 ratio (DPPC:DOPE:16-7NH-16) + 25  $\mu\text{g}$  of plasmid pAMAXA GFP DNA.  $n = 3$  for each group. Using a SoniGene 1 MHz probe microbubbles were destroyed in cell culture solution. Ultrasound intensities compared were 1.0  $\text{W}/\text{cm}^2$ , 1.5  $\text{W}/\text{cm}^2$ , and 2.0  $\text{W}/\text{cm}^2$

*Assessing ultrasound transfection capabilities in suspended HEK 293 cells*

Figure 18 illustrates cellular transfection of HEK 293 cells in suspension with gemini surfactant 16-7NH-16 microbubbles incorporated with ultrasound. The parameters of this investigation were modified to cells in suspension due to the lack of transfection expressed by cells attached to culture plate. Experimental groups investigated remained the same as previously investigated except for the addition of two experimental groups, neutral lipids + DOTAP MB + 25  $\mu$ g plasmid pAMAXA GFP DNA and 25  $\mu$ g plasmid pAMAXA GFP DNA + DOTAP MB. These two experimental groups were added for comparative purposes to gemini surfactant 16-7NH-16 MB + 25  $\mu$ g plasmid pAMAXA GFP DNA and are commercially used monovalent cationic lipids. After 48 hours of incubation cells were collected and counted for GFP expression. The results of this investigation illustrated the highest percent transfection was observed from positive control group Fugene + 25  $\mu$ g plasmid pAMAXA GFP DNA, with a 70 % transfection rate while not exposed to ultrasound. Experimental group 25  $\mu$ g plasmid pAMAXA GFP DNA + DOTAP MB illustrated transfection rates at 30 % and remained consistent between all ultrasound intensities, including control, not exposed to ultrasound. Experimental group neutral lipids + DOTAP MB + 25  $\mu$ g plasmid pAMAXA GFP DNA exhibited transfection rates which varied among ultrasound intensities; the highest transfection rate was observed from ultrasound intensity 2.0 W/cm<sup>2</sup> with a 30 % transfection rate. Gemini surfactant 16-7NH-16 MB + 25  $\mu$ g plasmid pAMAXA GFP DNA demonstrated a 5 % transfection rate among all ultrasound intensities tested and a zero transfection rate in control. Neutrally charged MB (negative control) demonstrated an increase in transfection rates with increasing ultrasound intensities; highest transfection rate was observed at intensity 2.0 W/cm<sup>2</sup> with a 12 % transfection rate.



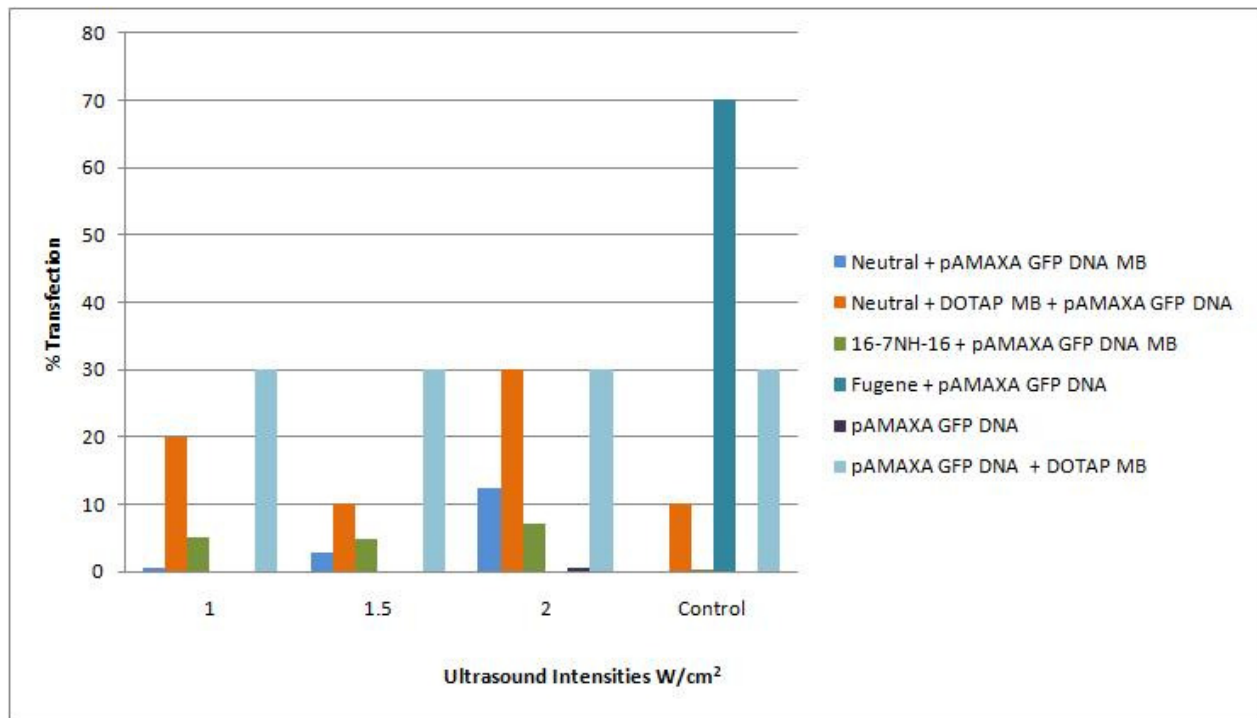


**Figure 16: Transfection efficiency comparison of pAMAXA plasmid GFP in suspended HEK 293 cells using ultrasound:** After 48 hours of incubation, cells were assessed for GFP expression. Positive control Fugene + 25  $\mu\text{g}$  of plasmid pAMAXA GFP DNA, Negative control neutral lipid microbubbles 10:1 ratio (DPPC:DOPE) + 25  $\mu\text{g}$  of plasmid pAMAXA GFP DNA, 25  $\mu\text{g}$  plasmid pAMAXA GFP DNA and 25  $\mu\text{g}$  plasmid pAMAXA GFP DNA + DOTAP were compared to experimental groups tested gemini surfactant 16-7NH-16 2:1 ratio (DPPC:DOPE:16-7NH-16) + 25  $\mu\text{g}$  of plasmid pAMAXA GFP DNA and neutrally charged lipid microbubbles 10:1 ratio (DPPC:DOPE) + DOTAP + 25  $\mu\text{g}$  of plasmid pAMAXA GFP DNA  $n = 3$  for each group. Using a SoniGene 1 MHz probe microbubbles were destroyed in cell culture solution. Ultrasound intensities compared were 1.0 W/cm<sup>2</sup>, 1.5 W/cm<sup>2</sup>, and 2.0 W/cm<sup>2</sup>

*Assessing ultrasound cell viability after transfection in suspended HEK 293 cells*

Figure 19 illustrates the estimated percent cell viability in transfected HEK 293 cells in suspension with ultrasound. The results indicate the highest percent cell death rate observed from experimental group 25  $\mu\text{g}$  plasmid pAMAXA GFP DNA + DOTAP MB (commercially used monovalent cationic lipid) with a percent death rate of approximately 90 %. This high cell death percentage was observed and maintained equally at all ultrasound intensities investigated, indicating ultrasound did not influence transfection rates from this experimental group. Experimental group 25  $\mu\text{g}$  plasmid pAMAXA GFP DNA (negative control) reached cell death rates equal to 25  $\mu\text{g}$  plasmid pAMAXA GFP DNA + DOTAP MB (90 %), although was only observed at ultrasound intensity 2.0  $\text{W}/\text{cm}^2$  and was not evident at any other ultrasound intensities. Neutral lipids + DOTAP MB + 25  $\mu\text{g}$  plasmid pAMAXA GFP DNA (commercially used monovalent cationic lipid) also exhibited high cell death rates reaching 90 % at ultrasound intensities 1.5  $\text{W}/\text{cm}^2$  and 2.0  $\text{W}/\text{cm}^2$ , indicating ultrasound influenced cell death with increasing intensities. Gemini surfactant 16-7NH-16 MB + 25  $\mu\text{g}$  plasmid pAMAXA GFP cell death rates was lower (68 %) when compared to commercially used monovalent cationic lipid DOTAP, ultrasound intensities influenced cell death rate with increasing ultrasound intensities from 1.0  $\text{W}/\text{cm}^2$  to 2.0  $\text{W}/\text{cm}^2$ , indicating the direct influence ultrasound had on cell death from this experimental group. Negative control group, neutrally charged MB, demonstrated comparable cellular death rates as gemini surfactant 16-7NH-16 MB + 25  $\mu\text{g}$  plasmid pAMAXA GFP DNA with increasing ultrasound intensities. The lowest percent cell death was observed from positive control group Fugene (commercially used monovalent cationic lipid) with cell death rates as low as 5 %.

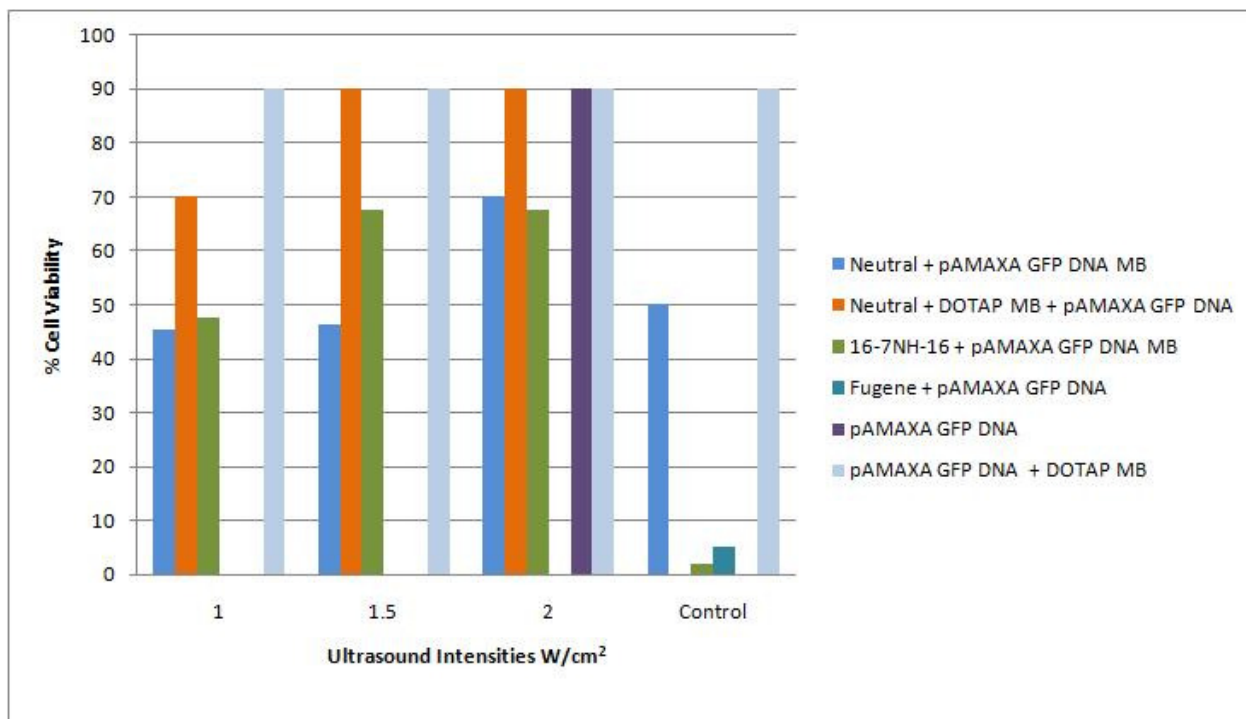


**Figure 17: Cell viability of transfected HEK 293 cells in suspension using ultrasound:** After 48 hours cell viability was assessed. Positive control Fugene + 25  $\mu$ g of plasmid pAMAXA GFP DNA, Negative control neutral lipid microbubbles 10:1 ratio (DPPC:DOPE) + 25  $\mu$ g of plasmid pAMAXA GFP DNA, 25  $\mu$ g plasmid pAMAXA GFP DNA and 25  $\mu$ g plasmid pAMAXA GFP DNA + DOTAP were compared to experimental groups tested gemini surfactant 16-7NH-16 2:1 ratio (DPPC:DOPE:16-7NH-16) + 25  $\mu$ g of plasmid pAMAXA GFP DNA and neutrally charged lipid microbubbles 10:1 ratio (DPPC:DOPE) + DOTAP + 25  $\mu$ g of plasmid pAMAXA GFP DNA  $n = 3$  for each group. Using a SoniGene 1 MHz probe microbubbles were destroyed in cell culture media. Ultrasound intensities compared were 1.0 W/cm<sup>2</sup>, 1.5 W/cm<sup>2</sup>, and 2.0 W/cm<sup>2</sup>

*Assessing ultrasound transfection capabilities of INS-1 832/13 cells in suspension*

A second cell line, INS-1 832/13, was used to test the transfection capabilities of gemini surfactant 16-7NH-16 incorporated with ultrasound. Figure 20 illustrates the results of cellular transfection of INS-1 832/13 cells with the incorporation of the ultrasound technique. The results indicated a zero transfection rate from all experimental groups tested. A minor transfection rate was indicated by negative control, neutrally charged MB + 25  $\mu$ g plasmid pAMAXA GFP DNA, at an intensity of 2.0 W/cm<sup>2</sup> with a 1 % transfection rate. Control groups not exposed to ultrasound demonstrated transfection rates of 40 % for both Lipofectamine 2000 MB + 25  $\mu$ g plasmid pAMAXA GFP DNA and 25  $\mu$ g plasmid pAMAXA GFP DNA. Gemini surfactant 16-7NH-16 MB + 25  $\mu$ g plasmid pAMAXA GFP DNA demonstrated a zero transfection rate at all ultrasound intensities investigated.

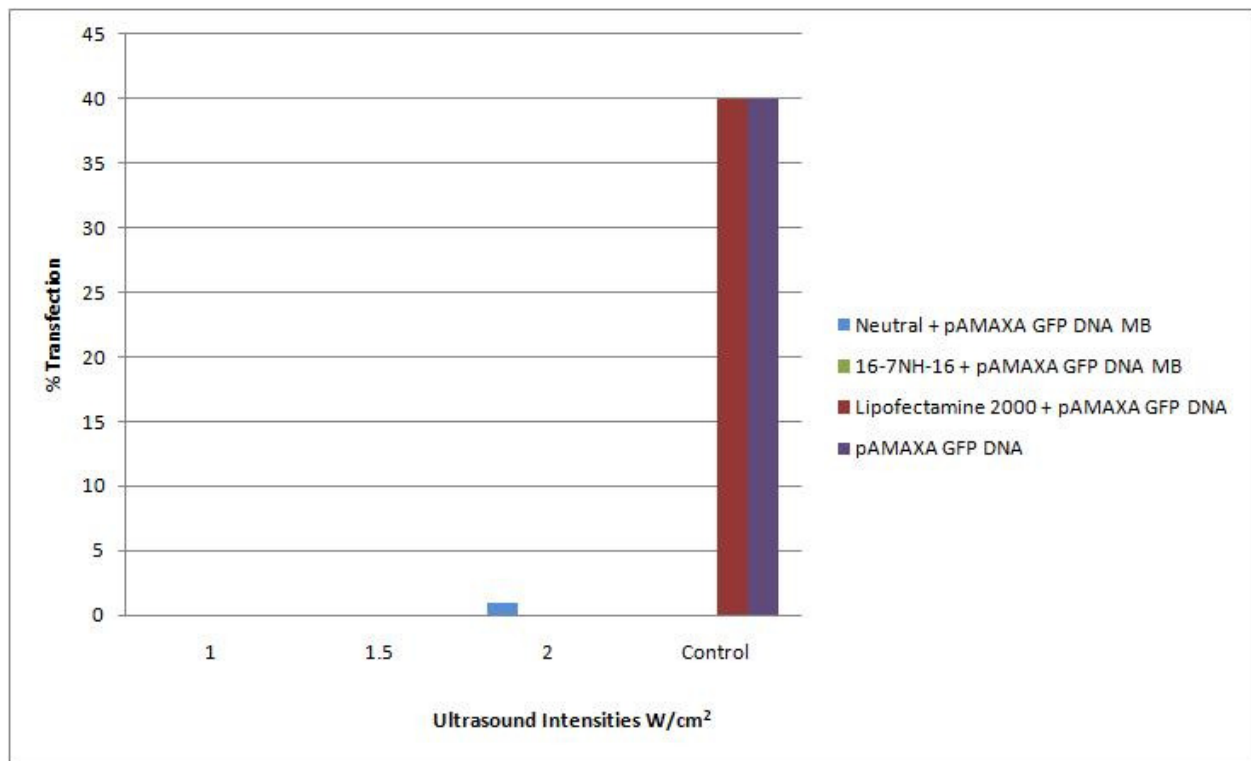


**Figure 18: Transfection efficiency comparison of pAMAXA plasmid GFP in suspended INS-1 832/13 cells using ultrasound:** After 48 hours cells assessed for GFP expression. Positive control Lipofectamine 2000 + 25  $\mu$ g of plasmid pAMAXA GFP DNA, Negative control neutral lipid microbubbles 10:1 ratio (DPPC:DOPE) + 25  $\mu$ g of plasmid pAMAXA GFP DNA and 25  $\mu$ g plasmid pAMAXA GFP DNA were compared to experimental group tested gemini surfactant 16-7NH-16 2:1 ratio (DPPC:DOPE:16-7NH-16) + 25  $\mu$ g of plasmid pAMAXA GFP DNA. n = 3 for each group. Using a SoniGene 1 MHz probe microbubbles were destroyed in cell culture solution. Ultrasound intensities compared were 1.0 W/cm<sup>2</sup>, 1.5 W/cm<sup>2</sup>, and 2.0 W/cm<sup>2</sup>.

*Assessing ultrasound cell viability after transfection in suspended INS-1 832/13 cells*

Figure 21 illustrates estimated cell viability in transfected INS-1 832/13 cells using ultrasound. The results indicate the highest percent cell death rate observed from experimental group gemini surfactant 16-7NH-16 MB + 25  $\mu$ g plasmid pAMAXA GFP DNA at a 90 % death rate, and was visible at all ultrasound intensities, including control group. All other experimental groups tested demonstrated little to no cellular death at all ultrasound intensities explored, except experimental group 25  $\mu$ g plasmid pAMAXA GFP DNA. Death rate was directly impacted by the increase in ultrasound intensities. As ultrasound intensities increased from 1.0 W/cm<sup>2</sup> to 2.0 W/cm<sup>2</sup> cellular death rates also increased; indicating the impact ultrasound exposure intensities has on cell death. Experimental group neutrally charged MB + 25  $\mu$ g plasmid pAMAXA GFP DNA (negative control) indicated a 1 % cell death rate at ultrasound intensity 2.0 W/cm<sup>2</sup> and not seen at any other ultrasound intensities. Positive control, Lipofectamine 2000 MB + 25  $\mu$ g resulted in a 5 % cell death with no ultrasound exposure.

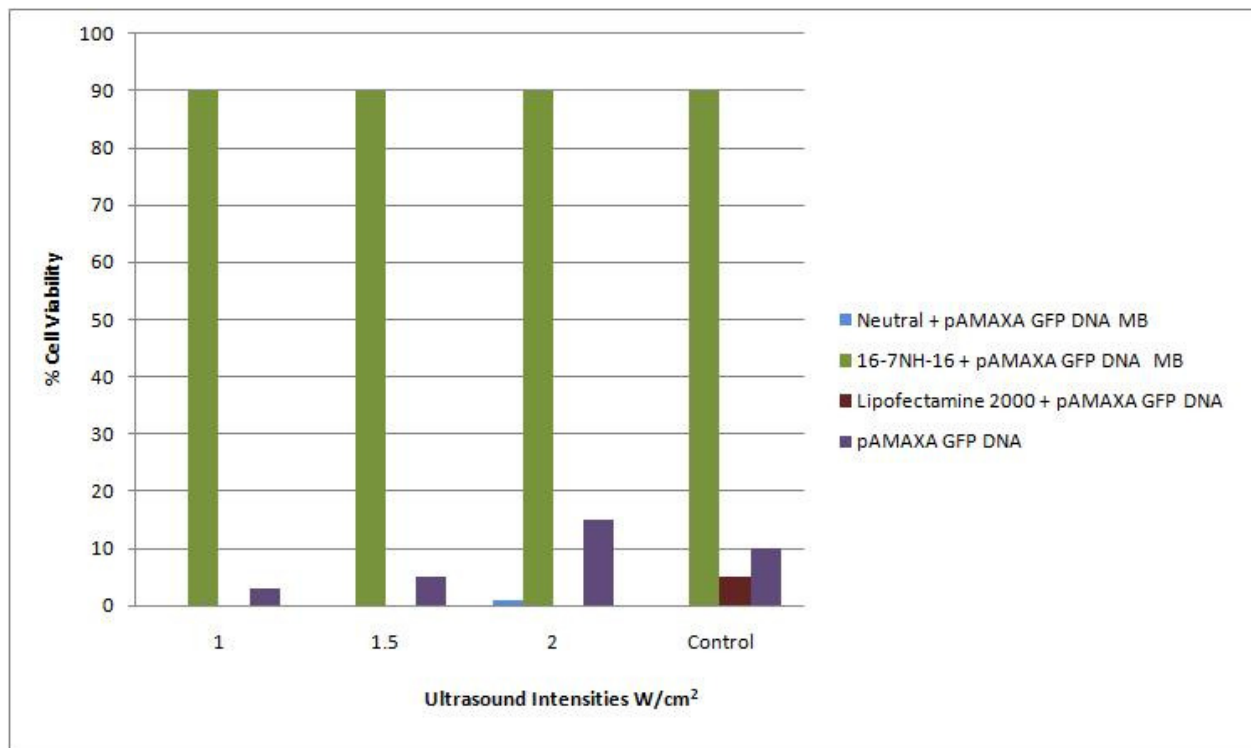


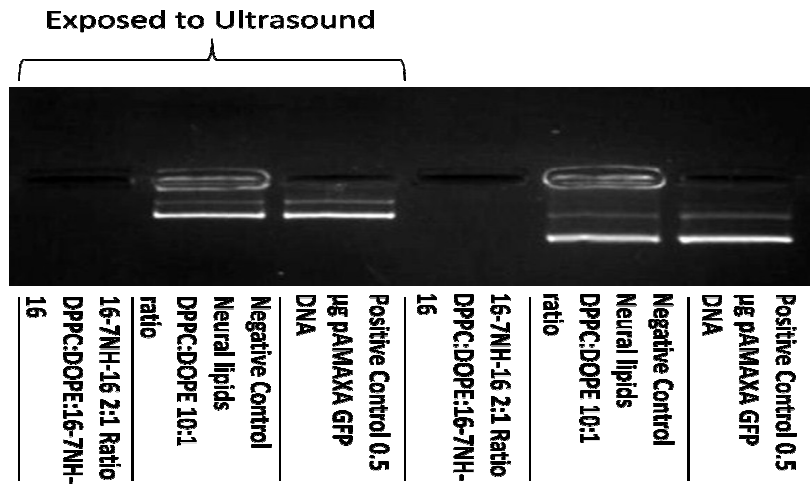
**Figure 19: Cell viability of transfected INS-1 832/13 cells in suspension using ultrasound:** After 48 hours cells were assessed for viability. Positive control Lipofectamine 2000 + 25  $\mu\text{g}$  of plasmid pAMAXA GFP DNA, Negative control neutral lipid microbubbles 10:1 ratio (DPPC:DOPE) + 25  $\mu\text{g}$  of plasmid pAMAXA GFP DNA and 25  $\mu\text{g}$  plasmid pAMAXA GFP DNA were compared to experimental group tested gemini surfactant 16-7NH-16 2:1 ratio (DPPC:DOPE:16-7NH-16) + 25  $\mu\text{g}$  of plasmid pAMAXA GFP DNA.  $n = 3$  for each group. Using a SoniGene 1 MHz probe microbubbles were destroyed in cell culture solution. Ultrasound intensities compared were 1.0  $\text{W}/\text{cm}^2$ , 1.5  $\text{W}/\text{cm}^2$ , and 2.0  $\text{W}/\text{cm}^2$

### *Assessing plasmid pAMAXA GFP DNA binding and release using ultrasound*

To achieve successful gene delivery using ultrasound, the cargo loaded onto the non-viral gene carrier must be released once exposed to ultrasound. Figure 15 **A** illustrates the results of the ultrasound release of 50 µg of plasmid pAMAXA GFP DNA from gemini surfactant 16-7NH-16 MB. Plasmid pAMAXA GFP DNA release was compared to 1) 50 µg plasmid pAMAXA GFP DNA (negative control), and 2) neutral lipid MB + 50 µg of plasmid pAMAXA GFP DNA (negative control). For comparative purposes, the first experimental group was synthesized and not exposed to ultrasound and seen in Figure 15 **A** lanes 4, 5, and 6. A second sample group was tested for plasmid pAMAXA GFP DNA release by ultrasound exposure. Lipid solutions were exposed to ultrasound for 30 seconds then loaded onto electrophoresis gel. The results indicate no difference between experimental groups exposed and not exposed to ultrasound with respect to plasmid pAMAXA GFP DNA release. Another experimental group was tested and is represented in Figure 15 **B**, using gemini surfactant 16-7NH-16 MB at a 10:1. Figure 15 **B** indicates a reduced binding capability of gemini surfactant 16-7NH-16 MB at a 10:1 rather than 2:1 ratio in both ultrasound exposed and not exposed groups. This was indicated by the small amount of plasmid DNA detected on the agarose gel. These results confirm ultrasound has no release effect on gemini surfactant 16-7NH-16 MB at either a 2:1 or 10:1 ratio of surfactant to neutral lipids.



A)



B)

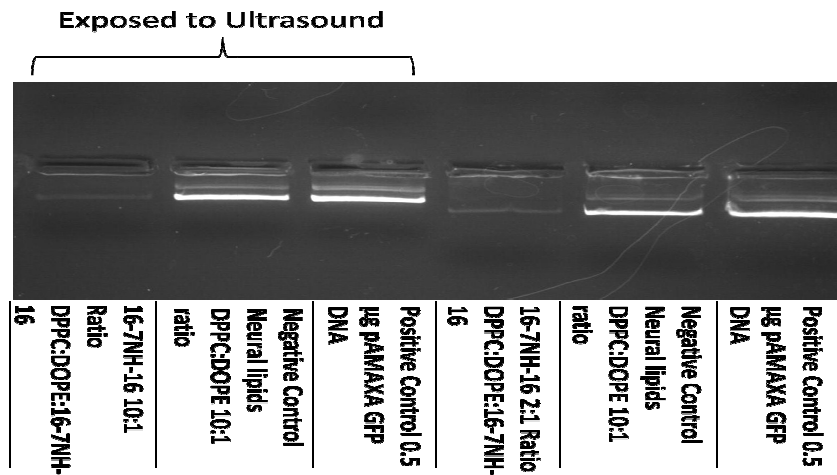


**Figure 20: Plasmid pAMAXA GFP DNA binding and release with ultrasound:** DNA condensing and release using ultrasound assessed by gel electrophoresis. Figure A) Positive control 50 µg pAMAXA GFP DNA, negative control neutral lipid microbubbles 10:1 ratio DPPC: DOPE + 50 µg pAMAXA GFP DNA. Experimental group gemini surfactant 16-7NH-16 2:1 ratio (DPPC:DOPE:16-7NH-16) + 50 µg pAMAXA GFP DNA. Microbubbles containing pAMAXA plasmid GFP DNA were exposed to ultrasound with a 1MHz SoniGene probe for 30 seconds then loaded onto a 1 % agarose gel. Figure B) DNA condensing and release assessed by gel electrophoresis. Control groups used remained the same, experimental group gemini surfactant 16-7NH-16 was reduced to a 10:1 ratio (DPPC:DOPE:16-7NH-16) + the addition of 50 µg pAMAXA GFP DNA. All experimental parameters stayed the same as seen in figure A.

### *Displacement of the Aqueous Center*

Displacement of the aqueous center is desired for efficient gene delivery when incorporated with ultrasound. The investigation into the displacement of the aqueous center of synthesized microbubbles suggests the methodology used to synthesize microbubbles is successful in achieving a gas filled center. Figure 11 illustrates the displacement of the aqueous center of neutrally charged microbubbles. Microbubbles were successfully targeted and destroyed using the SoniGene 1MHz probe. Only neutrally charged microbubbles were used to confirm this investigation.

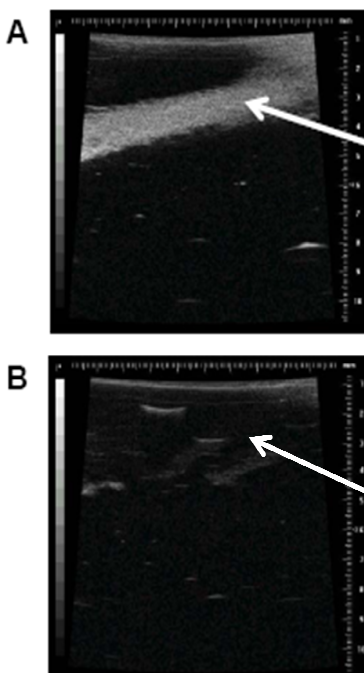


**Figure 21: Ultrasound Mediated Destruction of Neutral Gas Filled Microbubbles:** Destruction of neutral gas filled microbubbles with the 1MHz high frequency ultrasound probe and visualized using the Visual Sonics Vevo system. A) Neutral gas filled microbubbles were synthesized and injected into ultrasound gel using a 16 G needle (white streaks indicated by arrow). The microbubbles appear white likely because they are gas filled and reflect ultrasound waves. Ultrasound waves cannot pass through air, resulting in their reflection seen on the ultrasound image. B) Microbubbles were destroyed using pulse Visual Sonics SoniGene 1 MHz probe. This resulted in the destruction of the bubbles under the high frequency ultrasound and the release of the perfluorocarbon gas. This is indicated in figure B where the white streaks disappeared.

# Chapter 6

## 6.1 Discussion

The purpose of this study was to develop an optimized microbubble gene carrier using a new family of cationic lipids known as gemini surfactants to incorporate with the ultrasound delivery technique. Gemini surfactants have been recognized for their superior DNA binding capabilities, colloidal stability, increased transfection rates and for their economic advantages (Kirby et al., 2003; Wettig et al., 2007). Developing an optimized microbubble gene carrier using gemini surfactants to be incorporated with ultrasound would ultimately increase success rates for its *in vivo* and clinical application.

The first objective of this study was to assess microbubble particle size and charge (zeta potential) of gemini surfactants 16-3-16, 16-7NH-16 and compare them to monovalent cationic lipid Lipofectamine 2000. Investigating and determining particle size is important because administration of non-viral microbubble gene carriers is performed intravenously; these particles must acquire a small size while suspended in solution to allow lung clearance during circulation, safety without causing death by restricting small arterioles or blood vessels and requires total perfusion into a target tissue for *in vivo* application (Tinkov et al., 2008; Yoon et al., 2010; Kwon et al., 2008). Also, gene delivery into a target cell using ultrasound is thought to be induced by endocytosis. As a particle comes into contact with a cell's surface it facilitates endocytosis (Kirby et al., 2003; Zhdanov et al., 2001). This pathway can be restricted by large particles resulting in decreased transfection rates (Meijering et al., 2009). Assessing charge of a particle system provides information on the particles dispersion, colloidal stability, biological characteristics and drug/gene loading capacities (Tinkov et al., 2008). An increased surface charge results in longer capillary retention times while in circulation after intravenous administration. The attachment of drugs or genes onto a non-viral gene carrier is achieved through surface electrostatic interaction. Plasmid DNA holds a negative charge and requires a strong positively charged particle surface

for efficient DNA binding (Ma et al., 2007; Zhdanov et al., 2002; Gary et al., 2007; Alatorre-Meda et al., 2010). Predetermining size and charge of cationic particles prior to DNA loading gives insight for their use as non-viral gene carriers. Particle size and charge play dual roles in creating a stable non-viral gene delivery system.

When assessing particle size of gemini surfactant species 16-3-16 and 16-7NH-16 both surfactants achieved a smaller and more desirable particle size of 0.167  $\mu\text{m}$  for 16-3-16 and 0.275  $\mu\text{m}$  for surfactant 16-7NH-16 when compared to Lipofectamine 2000 (3.09  $\mu\text{m}$ ) prior to DNA loading. Gemini surfactants achieved a size between 1-8 $\mu\text{m}$ , which is safe for intravenous administration, organ perfusion and for facilitated cellular uptake (Thatte et al., 2005; Meijering et al., 2009). Particle surface charge, measured through zeta potential, revealed both gemini surfactants achieving a strong surface charge of +29 mV for gemini surfactant 16-3-16 and +30 mV for gemini surfactant 16-7NH-16 when compared to Lipofectamine 2000 (-6.2 mV). These values indicate that gemini surfactants achieved a greater stable colloidal system with quality dispersion properties, enough electrostatic repulsion between particles for intravenous administration for increased retention times, and sufficient DNA binding potential when compared to Lipofectamine 2000, where size and charge indicates an unsafe and unstable colloidal system.

It was hypothesized that gemini surfactants would achieve a smaller particle size with increased charge based on the additional spacer group. These results support this hypothesis since both gemini surfactants achieved a smaller particle size with increased surface charge when compared to the monovalent cationic lipid Lipofectamine 2000.

What makes gemini surfactants so unique compared to monovalent cationic lipids is the addition of a spacer group. This ridged spacer adds an additional amino group to be incorporated into its structure, providing an increased positive surface charge (Kirby et al., 2003; Wettig et al., 2007). As an increase in charge is achieved, there is an increase in repulsion between particles. It can be

suggested that the additional amino group not only increases a particles surface charge but also causes these particles to compact into smaller structures due to the flexibility of the spacer group as repulsion between particles is high. The results support both the hypothesis and previous literature of gemini surfactants' small size and superior surface charge due to the additional spacer group when compared to monovalent cationic lipid microbubbles (Wettig et al., 2003, Ewert et al, 2002).

The second objective of this study was to assess the effects DNA binding has on particle size and charge of gemini surfactants 16-3-16 and 16-7NH-16. Lipofectamine 2000 was no longer compared for DNA binding assessment due to the information provided by the results based on an increased particle size and reduced surface charge prior to DNA assessment. It is important to assess the effects DNA binding has on particles' size and charge to ensure DNA is interacting at the particles' surface for efficient gene delivery; and appropriate microbubble size parameters are being maintained for intravenous administration, a suitable size for cellular uptake, while still maintaining colloidal stability. The results of this investigation demonstrate that gemini surfactant 16-3-16 increased in particle size after the addition of DNA from 0.167  $\mu\text{m}$  to 2.23  $\mu\text{m}$  and gemini surfactant 16-7NH-16 increased in particle size from 0.275  $\mu\text{m}$  to 0.73  $\mu\text{m}$ . Particle surface charge, measured though zeta potential after the addition of DNA demonstrated that both gemini surfactant 16-3-16 and 16-7NH-16 increased in surface charge. Surfactant 16-3-16 increased from +34 mV to +39 mV and surfactant 16-7NH-16 increased from +34.6 mV to +37.74 mV.

It was hypothesized that a reduced particle size and reduced loss in surface charge would be achieved from gemini surfactants 16-7NH-16 after the addition of DNA due to the N-H *imino* group present within the spacer. These results support this hypothesis and gemini surfactant 16-7NH-16 achieved a reduced particle size while maintaining a high surface charge when compared to surfactant 16-3-16 after the addition of DNA.

DNA binding and condensing properties of gemini surfactants are directly correlated to spacer composition (Kirby et al., 2003). Two commonly used spacers groups, the *aza* and *imino* groups were investigated for their DNA binding potential and compacting capabilities. Previous studies have revealed that gemini surfactants which contain an N-H group have a strong DNA binding capacity, increased DNA binding affinity, and condensing and compaction properties (Wettig et al., 2007; Luciani et al., 2007). The *imino* group differs from the *aza* by an additional amino group present within the spacer. This results in an additional DNA binding site and increased surface charge. It can be concluded from these results that the additional N-H group present in the spacer allowed greater DNA condensing resulting in the reduced particle size of gemini surfactant 16-7NH-16. The additional *imino* N-H group present within the spacer can also influence charge. Prior to the addition of DNA, gemini surfactant 16-7NH-16 achieved a greater surface charge. Although after the addition of DNA both particle systems exhibited in a shift in a positive charge, to approximately  $+38$  mV. This shift in charge can be typical of a highly charge particle system. Literature has supported that as DNA interacts with the cationic compound, the negative charge can be reduced, diminished or even shift to a positive charge as the negative charge of DNA is neutralized by the positive charge of the liposome (Alatorre-Meda et al., 2010; Felgner et al., 1995). This coincides with the results in the increased positive surface charge observed by both gemini surfactants. These results indicated that gemini surfactant 16-7NH-16 achieved a smaller particle size after the addition of DNA maintaining appropriate parameters for intravenous administration, cellular uptake, while maintaining a strong surface charge. This investigation determined that DNA is affecting the particle system but does not confirm DNA surface binding. Further investigation was done using gel electrophoresis to determine surface interaction. Due to the superior surface compacting capabilities demonstrated by gemini surfactant 16-7NH-16 it was chosen for further surface DNA binding investigation.

The results in figure 14 confirm plasmid DNA surface binding to gemini surfactant 16-7NH-16 microbubbles. Gemini surfactant 16-7NH-16 was able to fully bind, and quenched plasmid DNA and was undetectable by ethidium bromide. Ethidium bromide is an intercalating agent used as a

fluorescent tag that binds to nucleic acids and is commonly used for gel electrophoresis. Surfactant 16-7NH-16 microbubbles were able to bind and condense DNA to such capacities that ethidium bromide was not able to penetrate or bind to the nucleic acids present on plasmid DNA. This investigation supports the strong binding and compacting capabilities of surfactant 16-7NH-16 which contains the N-H *imino* spacer group.

The third objective of this study was to assess transfection efficiencies and toxicity rates *in vitro* of gemini surfactant 16-7NH-16 microbubbles and to compare monovalent microbubbles with the incorporation of ultrasound. The importance of this investigation was to determine whether or not synthesized gemini surfactant 16-7NH-16 microbubbles can in fact transfect DNA at equal or higher rates with reduced toxicity into two cell lines with the incorporation of ultrasound to be used as non-viral microbubble gene carriers.

The results of the *in vitro* assessment revealed that gemini surfactant 16-7NH-16 microbubbles cannot transfect DNA at either equal or higher rates with reduced toxicity when compared to monovalent cationic microbubbles. Transfection rates of gemini surfactant 16-7NH-16 microbubbles in HEK 293 cells demonstrated a 5 % transfection rate with approximately a 68 to 90 % death rate. When compared to the monovalent cationic microbubbles, both Fugene and DOTAP exhibited the highest transfection rates between 100 % (Fugene) and 30 % (DOTAP) with the lowest death rate observed from Fugene at 0 %. DOTAP demonstrated a 90 % death rate when incorporated with ultrasound. When assessing transfection rates of gemini surfactant 16-7NH-16 microbubbles in INS-1 832/13 cells a 0 % transfection was observed and a 90 % death rate. This was compared to monovalent Lipofectamine 2000 microbubbles which exhibited a 40 % transfection rate and a 5 % death rate overall.

It was hypothesized that gemini surfactant 16-7NH-16 microbubbles would exhibit higher transfection rates with reduced toxicity based on its reduced particle size, colloidal stability, dispersion properties and its increased DNA binding capabilities demonstrated by the additional



N-H *imino* group. The results of this investigation did not support the hypothesis, despite the encouraging results presented by surfactant 16-7NH-16 during the previous investigations. Overall, monovalent cationic lipid microbubbles demonstrated not only higher transfection rates, but also exhibited lower toxicity rates when compared to gemini surfactant 16-7NH-16.

The lack of transfection observed by gemini surfactant 16-7NH-16 microbubbles coincides with the high toxicity rates observed in both cell lines. There are several possible reasons for the lack of transfection such as cytotoxicity and exposure to high frequency ultrasound. Ultrasound is known to enhance transfection rates by facilitating the uptake of particles into a target cell (Meijering et al., 2009; Unger et al., 2001; Pitt et al., 2004). It has been established that the uptake of large quantities of cationic lipids can result in cell death due to toxicity (Ewert, et al., 2002). It is plausible that the highly charged gemini surfactants together with ultrasound resulted in an increased particle uptake causing toxicity to the cells. Ultrasound frequencies used in this investigation were heavily increased for *in vitro* use. Several studies have used reduced ultrasound frequencies when delivering plasmid GFP to culture cells (Wang et al., 2008; Zhou et al., 2009). Reducing the surfactant to neutral lipid ratio, and ultrasound frequencies could reduce cellular death rates and increase cellular transfection. Literature has shown support to increasing transfection rates with more neutral particles by increasing the addition of neutral lipids (co-helper lipids) to cationic lipids resulting in lower toxicity and increased transfection rates (Gary et al., 2007; Ewert, et al., 2002; Borden et al., 2005; Alatorre-Meda, et al., 2010). This can be a contradictory concept considering the theory behind DNA binding, complexing with lipid structures and cellular membrane charge. Much research has been dedicated to understanding how these complexes work and understanding the structure they form when complexed with DNA. Research has indicated that the amount of neutral lipid applied to the molar ratio will affect the structure a lipoplex will form as well as transfection rates (Alatorre-Meda et al., 2010). One study investigated transfection efficiencies when changing the mass ratio of cationic lipids to neutral. This study observed a dramatic increase in transfection efficiencies as the amount of cationic lipid was reduced from 50 to 20 mol % and the neutral lipid ratio increased (Ewert, et al.,

2002; Alatorre–Meda, et al., 2010). This drastic increase in transfection rates as neutral lipids are increased is particularly evident when using multivalent cationic lipids (Ewert, et al., 2002; Zhi et al., 2010). Further investigation must be done to confirm whether or not gemini surfactants can deliver nucleic acid for gene therapy efficiently when incorporated with ultrasound. This study did not fully explore all the experimental possibilities during the transfection process using ultrasound. Although it was previously determined that monovalent cationic lipid microbubbles demonstrated large particle size and reduced charge indicating an unstable system, our *in vitro* assessment determined monovalent cationic lipid microbubbles are more efficient gene carriers when incorporated with the ultrasound technique.

The lack of transfection observed from gemini surfactant 16-7NH-16 microbubbles was confusing despite the encouraging results presented and supported by each hypothesis. Gene delivery using the ultrasound technique does require the release of its cargo from the cationic lipid to be transfection and expressed within the cell. It is plausible that perhaps the lack of transfection observed from gemini surfactant 16-7NH-16 was a result of the DNA not released from the lipid during ultrasound exposure. Previous investigations determined that DNA was interacting with the gemini surfactant microbubble surface after DNA addition by increasing in particle size, increasing surface charge, and confirmation though gel electrophoresis. It can therefore be hypothesized that a reduction in transfection rates will be observed from transfection reagents who's cargo cannot be released during ultrasound exposure.

The results seen in figure 21 confirm gemini surfactant 16-7NH-16 was unable to release DNA after ultrasound exposure and support this hypothesis. Gemini surfactant 16-7NH-16 microbubbles were synthesized at a 2:1 ratio and were chosen for investigation based the results of previous investigations demonstrating a small particle size, increase surface charge and DNA binding capabilities. These results suggest that the 2:1 ratio used might bind plasmid DNA with such strong forces that ultrasound may not be able to successfully release plasmid DNA from its structure. Research has supported that the electrostatic binding between DNA and cationic lipids

may be so strong that DNA cannot be released during the appropriate stage, resulting in low levels of gene expression (Gary, et al., 2007). Neutral lipid microbubbles have a reduced ability to bind DNA (Figure 14). It is predicted that an increase in the amount of neutral lipids could reduce the DNA binding and condensing capabilities of surfactant 16-7NH-16 microbubbles to help facilitate the release with the incorporation of ultrasound, resulting in higher transfection rates *in vitro*. Although, not included in the study objectives, and after the observation of DNA not released from gemini surfactant 16-7NH-16 microbubbles, it was suggested that perhaps the aqueous center of synthesized microbubbles was not being displaced by the perfluorocarbon gas. To confirm the methodology used to displace the aqueous center of synthesized gemini surfactant microbubbles both visual and high frequency ultrasound were used to confirm methodology. Gene delivery using ultrasound requires a gas filled microbubble center for microbubble explosion to deliver its contents (Thatte et al., 2005; Tinkov et al., 2008; Unger et al., 2002, Djkmans et al., 2004). It is hypothesized that obtaining a microbubble gas filled center and when exposed to high frequency ultrasound will result in its destruction. It is important to ensure the methodology used for microbubble synthesis is correct in achieving the acquired conditions to be incorporated with ultrasound for efficient gene delivery using this technique.

The results seen in figure 11 confirm and support the hypothesis that a gas filled microbubble center is achieved and is destroyed when exposed to high frequency ultrasound. Therefore with respect to the lack of transfection observed by gemini surfactant 16-7NH-16 *in vitro*, this was not due to the methodology used in achieving a gas filled center. It must be stated that only neutral lipids were used to confirm this methodology. Since gemini surfactants were not used to confirm a gas filled center it cannot be fully concluded that synthesized gemini surfactant microbubbles were actually achieving the required conditions, however, the methodology used does generate the appropriate microbubble conditions for ultrasound destruction.

### *Summary*

The costs of monovalent cationic lipids are quite high, resulting in economic drain for their clinical use. Gemini surfactants would be an ideal transfection reagent to be used when incorporated with the UTMD technique for treatment based on their low cost and the reduced amount of surfactant compound required to bind DNA. This is quite attractive for their *in vivo* use by increasing safety during application and their economic advantages. Further detailed investigation and studies are required to determine if gemini surfactants could be incorporated with the UTMD technique. Ideally, low cost, easy production, high transfection capabilities, lack of immunogenicity, low toxicity are the most sought out principles when developing non-viral gene carriers. Cationic lipids for gene delivery have been taken to the stage of clinical trials, although the efficiency of synthetic vectors still needs to be greatly improved as demonstrated during the investigation of this study. With the increasing success using UTMD as a gene delivery system, UTMD holds great promise as a potential gene delivery system to improve the treatment of islet transplantation. More sufficient investigation and optimization is required, although its potential holds great promise to treat disease.

### *Conclusion*

In conclusion to this study, it was determined through detailed investigation that the most appropriate microbubble gene carriers to be incorporated with ultrasound for gene delivery for *in vitro* cell culture are the monovalent cationic lipids. This is the first investigation known to use gemini surfactants to synthesize microbubble gene carriers and incorporate them using this technique. Unfortunately, *in vitro* assessment of the investigation of gemini surfactants illustrated negative results reducing their use as microbubble gene carriers to be incorporated with the UTMD technique.

### *Future Directions*

Gene therapy holds great promise to treat a variety of human diseases, including diabetes. Diabetes is a devastating disease affecting millions of people worldwide, ultimately reducing the quality of life. Current treatments are available to help alleviate this burden but the quality of life for diabetics is still compromised. Diabetics are continuously faced with an uphill battle and constant reminders of future secondary complications which can impede their life and in some cases leading to premature death. The development of the artificial pancreas is a fast developing alternative treatment, although many drawbacks still impede its progression and diabetics are burdened by surgical implantation and the carrying an insulin pump at all times. Ultimately, islet transplantation is the ideal form of treatment for diabetics. This form of treatment alleviates diabetics from constant self-monitoring and carrying devices upon which they are dependent. Islet transplantation as a form of treatment for diabetes would allow diabetics to live an insulin independent life without the burden of secondary complications. The success of the “Edmonton Protocol” catapulted research into a possible cure (Bretzel et al., 2007; Shapior et al., 2006; Yones et al., 2008; Halban et al., 2010). Although, limitations such as islet supply, survival and immunosuppression impede its progression. The characterization of genes that either enhance  $\beta$ -cell functionality, islet revascularization or increase  $\beta$ -cell mass either through controlled proliferation, transdifferentiation or neogenesis, holds great promise for the application of gene therapy as a treatment for diabetes. Initial experiments with viral vectors have highlighted the shortcoming of this strategy. The cytotoxic and immunogenic nature of the viral gene carriers has urged the need to develop a more effective non-viral gene delivery method, such as UTMD. The organ-specific application of a ultrasound pulse, which not only initiates cargo release, but also facilitates the cargo uptake by the target cells, indicates that UTMD is particularly well suited for the pancreatic delivery of a combination of genes that will increase functional  $\beta$ -cell mass and the revascularization post islet transplantation (Chen et al., 2010; Shimoda et al., 2010). Further and future investigation into designing a more cost efficient microbubble gene carrier to be incorporated with ultrasound could cure diabetes and many other inherited diseases.

## Bibliography

- Alatorre-Meda, M., Gonzalez-Perez, A., Rodriguez, J., 2010. DNA-Metafectene Pro Complexation: a physical chemistry study. *Physical Chemistry Chemical Physics*. (10)1039/b92900j
- Ashcroft, F. M., Rorsman, P., 1989. Electrophysiology of the pancreatic beta-cell. *Prog Biophys Mol Biol* 54(2):87-143
- Bekeredjian, R., Bohris, C., Hansen, A., Katus, H. A., Kuecherer, H. F., & Hardt, S. E., 2007. Impact of microbubbles on shock wave-mediated DNA uptake in cells in vitro.
- Bekeredjian, R., Chen, S. Y., Frenkel, P. A., Grayburn, P. A., & Shohet, R. V., 2003. Ultrasound-targeted microbubble destruction can repeatedly direct highly specific plasmid expression to the heart. *Circulation*, 108(8), 1022-1026.
- Bekeredjian, R., Kroll, R. D., Fein, E., Tinkov, S., Coester, C., Winter, G., 2007. Ultrasound targeted microbubble destruction increases capillary permeability in hepatomas. *Ultrasound In Medicine And Biology*, 33(10), 1592-1598.
- Bonner-Weir, S., 2000. Life and death of the pancreatic beta cells. *Trends Endocrinol Metab* 11:375-378
- Borden, M. A., Kruse, D. E., Caskey, C. F., Zhao, S. K., Dayton, P. A., & Ferrara, K. W., 2005. Influence of lipid shell physicochemical properties on ultrasound-induced microbubble destruction.
- Borden MA., Caskey CF, Little E, Gillies RJ, Ferrara KW., 2007. DNA and polylysine absorption and multilayer constructs into cationic lipid-coated microbubbles. *Langmuir*. 23(18):9401-8.
- Boucher, A., Lu, D., Burgess, S.C., Telemaque-Potts, S., Jensen, M.V., Mulder, H, Wang, M.Y., Unger, R.H., Sherry, A.D., Newgard, C.B., 2004. *Long-chain coA esters activate human pancreatic beta-cell KATP channels: potential role in Type 2 diabetes*. *Diabetologia* 47:277-283
- Bretzel, R. G., Jahr, H., Eckhard, M., Martin, I., Winter, D., Brendel, M. D., 2007. Islet cell transplantation today. *Arch Surg*, 392:239-253
- Brunnicardi, FC, Stagner, J, Bonner-Weir, S, Wayland, H, Kleinman, R, Livingston, E, Guth, P, Menger, M, Mccuskey, R, Intaglietta, M, Charles, A, Ashley, S, Cheung, A, Ipp, E, Gilman, S, Howard, T, Passaro, E Jr., 1996. Microcirculation of the islets of Langerhans. Long beach veterans administration regional medical education center symposium. *Diabetes* 45:385-92

Caracciolo, Giulio. 2005. Do CD-Chol/DOPE-DNA complexes really form an inverted hexagonal phase? *American Journal of Biochemistry*.

Casatano, L., Eisenbarth, G., 1990. A Chronic Autoimmune Disease of Human, Mouse, and Rat. *Annual Review Immunology*, 8:647-679

Chee, W., Saudek, D., 2004. Glucose sensors: toward closed loop insulin delivery. *Journal of Endocrinology and Metabolism* 33:175-195

Chen, S. Y., Ding, J. H., Bekeredjian, R., Yang, B. Z., Shohet, R. V., Johnston, S. A., et al. (2006). Efficient gene delivery to pancreatic islets with ultrasonic microbubble destruction technology. *Proceedings of the National Academy of Sciences of the United States of America*, 103(22), 8469-8474.

Chen. S., Shimoda, M., Wang, M.Y., 2010. Regeneration of pancreatic islets in vivo by ultrasound-targeted gene therapy. *Gene Therapy* 1-10.

Colom, C., Corcoy, R., 2010. Maturity onset diabetes of the young and pregnancy. *Best Practice & Research Clinical Endocrinology & Metabolism* 24: 605–615

Christiansen, J. P., French, B. A., Klibanov, A. L., Kaul, S., & Lindner, J. R., 2003. Targeted tissue transfection with ultrasound destruction of plasmid-bearing cationic microbubbles. *Ultrasound in Med. & Biol.*, 29(12):1759–1767.

Cook, D. L., Hales, C. N., 1984. Intracellular ATP directly blocks K<sup>+</sup> channels in pancreatic B-cells. *Nature* 311(5983): 271-3.

Creatore M., Moineddin R., Booth G., Manuel D., DesMeules M., McDermott S., Glazier R. 2010. Age- and sex-related prevalence of diabetes mellitus among immigrants to Ontario, Canada. *CMAJ*. 182 (8): 781-789.

Davis, M., 2002. Non-viral gene delivery systems. *Biotechnology* 13:128-131.

Dean, P. M., Matthews, E. K., 1970. Electrical activity in pancreatic islet cells: effect of ions. *J Physiol* 210(2):265-75.

Dijkmans, P. A., Juffermans, L. J. M., Musters, R. J. P., van Wamel, A., ten Cate, F. J., van Gilst, W., et al. (2004). Microbubbles and ultrasound: From diagnosis to therapy. *European Journal of Echocardiography: The Journal of the Working Group on Echocardiography of the European Society of Cardiology*, 5(4), 245-256.

Ewert, K., Ahmad, A., Evans, H., 2002. Efficient Synthesis and Cell-Transfection Properties of a New Multivalent Cationic Lipid for Nonviral Gene Delivery. *J. Med. Chem* 45:5023-5029.

Fallon, M. J., MacDonald, M. J., 2008. Beta-cell alpha-ketoglutarate hydroxylases may acutely participate in insulin secretion. *Metabolism* 57(8): 1148-54.

Felgner PL, Tsai YJ, Sukhu L, Wheeler CJ, Manthorpe M, Marshall J, Cheng SH. 1995. Improved cationic lipid formulations for in vivo gene therapy. *Ann N Y Acad Sci.* 772:126-39.

Feril, L. B., Ogawa, R., Kobayashi, H., Kikuchi, H., & Kondo, T., 2005. Ultrasound enhances liposome-mediated gene transfection. *Ultrasonics Sonochemistry*, 12(6), 489-493.

Ferrannini, E., 1998. Insulin resistance versus insulin deficiency in non-insulin-dependent diabetes mellitus: problems and prospects. *Endocrine Review.* 19:477-490.

Flamez, D., Berger, V., Kruhoffer, M., Orntoft, T., Pipeleers, D., Schuit, F. C. 2002. Critical role for cataplerosis via citrate in glucose-regulated insulin release. *Diabetes* 51(7): 2018-24.

Gary, D. J., Puri, N., Wong, Y.Y., 2007. Polymer-based siRNA delivery: Perspectives on the fundamental and phenomenological distinctions from polymer-based DNA Delivery. *Journal of Controlled Release* 121: 64-73

Gembal, M., Gilon, P., Henquin, J. C., 1992. Evidence that glucose can control insulin release independently from its action on ATP-sensitive K<sup>+</sup> channels in mouse B cells. *J Clin Invest* 89(4): 1288-95.

Halban, P.A., German, M.S., Kahn, S.E., 2010. Current Status of Islet Cell Replacement and Regeneration Therapy. *Journal of Clin Endocrinol Metab*, 95(3):1034-1043.

Hara, Y., Fujino, M., Nakada, K., Kimura, K., Adachi, K., & Li, X., 2006. Influence of the numbers of islets on the models of rat syngeneic-islet and allogeneic-islet transplantations. *Transplantation Proceedings*, 38(8), 2726-2728.

Heilbronn, R., Weger, S., 2010. Viral Vectors for Gene Transfer: Current Status for Gene Therapeutics. *Handb Exp Pharmacol.*(197):143-70.

Hellman, B., Gylfe, E., Wesslen, N., Hallberg, A., Grapengiesser, E., Marcstrom, A., 1994. Plasma membrane associated ATP as a regulator of the secretory activity of the pancreatic beta-cell. *Diabetologia* 37 Suppl 2: S11-20.

Henquin, J. C., 1998. A minimum of fuel is necessary for tolbutamide to mimic the effects of glucose on electrical activity in pancreatic beta-cells. *Endocrinology* 139: 993-8



Henquin, J.C., 2000. The triggering and amplifying pathways of the regulation of insulin secretion by glucose. *Diabetes* 49:1751-1760.

Henquin, J. C., Ravier, M. A., Nenquin, M., Jonas, J. C., Gilon, P., 2003. Hierarchy of the beta-cell signals controlling insulin secretion. *Eur J Clin Invest* 33(9):742-50.

Henquin, J. C., Nenquin, M., Ravier, M. A., Szollosi, A. 2009. Shortcomings of current models of glucose-induced insulin secretion. *Diabetes Obes Metab* 11: 168-179

Henquin, J.C., 2009. Regulation of insulin secretion: a matter of phase control and amplitude modulation. *Diabetologia* 52:739-751

Hoekstra, D., Rejman, J., Wasungu, L., Shi, F., & Zuhorn, I., 2007. Gene delivery by cationic lipids: In and out of an endosome. *Biochemical Society Transactions*, 35(1), 68-71.

Hou JC, Min L., Pessin JE., 2009. Insulin granule biogenesis, trafficking and exocytosis. *Vitam Horm.* 80:473-506.

Jacobson, D. A., & Philipson, L. H. (2007). Action potentials and insulin secretion: New insights into the role of kv channels. *DIABETES OBESITY & METABOLISM*, 9, 89-98.

Jeffrey, F.M., Storey, C.J., Sherry, A.D., 1996. <sup>13</sup>C NMR isotopomer model for estimation of anaplerotic substrate oxidation via acetyl-CoA. *Am J. Physiol Endocrinol Metab* 271:E788-E799

Juffermans, L. J. M., Dijkmans, P.A., Transient permeabilization of cell membranes by ultrasound-exposed microbubbles is related to formation of hydrogen peroxide. *Am J Physiol Heart Circ Physiol* 291: H1595-H1601

Jensen, M., Joseph, J., Ronnebaum, S., 2008. Metabolic cycling in control of glucose-stimulated insulin secretion. *Am J Physiol Endocrinol Metab* 295: E1287-E1297.

Jitrapakdee S., Wutthisathapornchai A., Wallace J.C., MacDonald M.J., 2010. Regulation of insulin secretion: role of mitochondrial signalling. *Diabetologia*, 53:1019-1032.

Joseph, J. W., Jensen, M. V., Ilkayeva, O., Palmieri, F., Alarcon, C., Rhodes, C. J., Newgard, C. B., 2006. The mitochondrial citrate/isocitrate carrier plays a regulatory role in glucose-stimulated insulin secretion. *J Biol Chem* 281(47): 35624-32.

Juvenile Diabetes Research Foundation [www.jdrf.ca](http://www.jdrf.ca)

Karp, Gerald. 2003. Cell and Molecular Biology

Kenmochi, T., Maruyama, M., Saigo, K., Akutsu, N., Iwashita, C., Otsuki, K., Ito, T., Suzuki, A., Miyazaki, M., Saito, T., 2008. Successful islet transplantation from the pancreata of non-heart-beating donors. *Transplantation Proceedings*, 40:2568-2570.

Kheirilomoom A, Ferrara KW., 2007. Cholesterol transport from liposomal delivery vehicles. *Biomaterials*.(29):4311-20. Epub 2007 Jul 3.

Kirby, A. J., Camilleri, P., Engberts, J.B.F., Feiters, M.C., 2003. Gemini Surfactants: New Synthetic Vectors for Gene Transfection. *Gene Transfection Agents* 42, 1448-1457.

Kwon, S. M., Nam, H. Y., Nam, T., Park, K., Lee, S., Kim, K., 2008. In vivo time-dependent gene expression of cationic lipid-based emulsion as a stable and biocompatible non-viral gene carrier. *Journal of Controlled Release* 128: 89–97.

Lindner, J. R., 2004. Microbubbles in medical imaging: Current applications and future directions. *Nature Reviews Drug Discovery* 3: 527-533.

Ludwig B, Zimerman B, Steffen A, Yavriants K, Azarov D, Reichel A, Vardi P, German T, Shabtay N, Rotem A, Evron Y, Neufeld T, Mimon S, Ludwig S, Brendel MD, Bornstein SR, Barkai U. 2010. A novel device for islet transplantation providing immune protection and oxygen supply. *Horm Metab Res*.

Lue, D., Mulder, H., Zhao, P., Burgess, S.C., Jensen, M.V., Kamzolova, S., Newgard C.B, Sherry, A.D., 2002. <sup>13</sup>C NMR isotopomer analysis reveals a connection between pyruvate cycling and glucose-stimulated insulin secretion (GSIS). *Proc Natl Acad Sci USA* 99:2708-2713.

Lu, H., Koshkin,C., Allister, E., 2010 Molecular and Metabolic Evidence for Mitochondrial Defects Associated with  $\beta$ -cell dysfunction in a mouse model of type 2 diabetes. *Diabetes* 59:448-459.

Luciani, P., Bombelli C., Colone, M., Giansanti, L., 2007. Influence of the Spacer of Cationic Gemini Amphiphiles on the Hydration of Lipoplexes. *Biomacromolecules* 8: 1999-2003

Ma, B. C., Zhang, S. B., Jiang, H. M., Zhao, B. D., & Lv, H. T., 2007. Lipoplex morphologies and their influences on transfection efficiency in gene delivery. *Journal of Controlled Release*, 123(3), 184-194.

MacDonald, M. J., 1995. Feasibility of a mitochondrial pyruvate malate shuttle in pancreatic islets. Further implication of cytosolic NADPH in insulin secretion. *J Biol Chem* 270(34): 20051-8.

MacDonald, M. J., 1995. Influence of glucose on pyruvate carboxylase expression in pancreatic islets. *Arch Biochem Biophys* 319(1): 128-32.

MacDonald, M. J., 1993. Estimates of glycolysis, pyruvate (de)carboxylation, pentose phosphate pathway, and methyl succinate metabolism in incapacitated pancreatic islets. *Arch Biochem Biophys*. 305:2 205-14.

MacDonald, M. J., 2002. Differences between mouse and rat pancreatic islets: succinate responsiveness, malic enzyme, and anaplerosis. *Am J Physiol Endocrinol Metab* 283(2): E302-10.

MacDonald, P. E., Joseph, J. W., & Rorsman, P., 2005. Glucose-sensing mechanisms in pancreatic beta-cells. *PHILOSOPHICAL TRANSACTIONS OF THE ROYAL SOCIETY B-BIOLOGICAL SCIENCES*, 360(1464), 2211-2225.

Maechler, P., Carobbio, S., Rubi, B., 2006. In beta-cells, mitochondria integrate and generate metabolic signals controlling insulin secretion. *Int J Biochem Cell Biol* 38:5-6.

Maechler, P., Wollheim, B., 1999. Mitochondrial glutamate acts as a messenger in glucose-induced insulin exocytosis. *Nature*, 402:685-689.

Marieb, E.N., Hoehn, K., 2007. Human Anatomy & Physiology Seventh Edition

Mayer, C. R., & Bekeredjian, R., 2008. Ultrasonic gene and drug delivery to the cardiovascular system. *Advanced Drug Delivery Reviews* 60:1177-1192.

Mayer, C. R., Geis, N. A., Katus, H. A., & Bekeredjian, R., 2008. Ultrasound targeted microbubble destruction for drug and gene delivery. *Expert Opinion on Drug Delivery*, 5(10), 1121-1138.

Mears, D., 2004. Regulation of insulin secretion in islets of langerhans by ca super(2+) channels. *Journal of Membrane Biology*, 200(2), 57-66.

Meglsson, M.D., Matschinsky, F.M., 1986. Pancreatic islet glucose metabolism and regulation of insulin secretion. *Diabetes Metab Rev* 2: 163-214.

Meijering, B. D. M., Juffermans, L. J. M., van Wamel, A., Henning, R. H., Zuhorn, I. S., Emmer, M., 2009. Ultrasound and microbubble-targeted delivery of macromolecules is regulated by induction of endocytosis and pore formation. *Circulation Research*, 104(5), 679-687.

Nenquin, M., Szollosi, A., Aguilar-Bryan, L., Bryan, J., Henquin, J. C., 2004. Both triggering and amplifying pathways contribute to fuel-induced insulin secretion in the absence of sulfonylurea receptor-1 in pancreatic beta-cells. *279(31):32316-24*.

Nesher, R., Cerasi, E., 2002. Modeling phasic insulin release: immediate and time-dependent effects of glucose. *Diabetes 51 Suppl 1: S53-9*.

Newgard, C. B., Lu, D., Jensen, M. V., Schissler, J., Boucher, A., Burgess, S., Sherry, A. D., 2002. Stimulus/secretion coupling factors in glucose-stimulated insulin secretion: insights gained from a multidisciplinary approach. *51 Suppl 3: S389-93*.

Newgard, C.B., Matschinsky, F.M., 2001. Substrate control of insulin release. In:*Handbook of Physiology, edited by J Jefferson A.C., Oxford, UK: Oxford Univ. Press, 125-152*

Newgard, C.B., McGarry J.D., 1995. Metabolic coupling factors in pancreatic beta-cell signal transduction. *Annu Rev Biochem 64: 689-719*.

Newsholme P., Gaudel C., McClenaghan NH., 2010. Nutrient regulation of insulin secretion and  $\beta$ -cell functional and integrity. *Adv. Exp. Med. Biol. 654:91-114*.

Ogawa, Y., Noma, Y., Davalli, A. M., Wu, Y. J., Thorens, B., Bonner-Weir, S., Weir, G. C., 1995. Loss of glucose-induced insulin secretion and GLUT2 expression in transplanted beta-cells. *Diabetes 44(1):75-9*.

Ohlerth, S., & O'Brien, R. T., 2007. Contrast ultrasound: General principles and veterinary clinical applications. *Veterinary Journal (London, England : 1997), 174(3), 501-512*.

Oliver-Krasinski, J. M., & Stoffers, D. A., 2008. On the origin of the beta cell.

Orci, L, Unger, R.H., 1975. Functional subdivision of islets of Langerhans and possible role of D cells. *Lancet 2:1243-4*.

Pantel, U., Schwanstecher, M., Wallasch, A., Lenzen, S., 1988. Glucose both inhibits and stimulates insulin secretion from isolated pancreatic islets exposed to maximally effective concentrations of sulfonylureas. *Naunyn Schmiedegeers Arch Pharmacol 338:459-462*

Pfeifer, M.A., Halter, J.B., Porte, D Jr., 1981. Insulin secretion in diabetes mellitus *Am J Med 70: 579-588*.

Pitt, W. G., Hussein, G. A., & Staples, B. J., 2004. Ultrasonic drug delivery--a general review. *Expert Opinion on Drug Delivery, 1(1), 37-56*.

Prentki, M., Matschinsky, F. M., 1987. Ca<sup>2+</sup>, cAMP, and phospholipid-derived messengers in coupling mechanisms of insulin secretion. *Physiol Rev* 67(4): 1185-248

Prentki M, Joly E, El Assaad W, Roduit R., 2002. Malonyl-CoA signaling, lipid partitioning, and glucolipotoxicity: role in betacell adaptation and failure in the etiology of diabetes. *Diabetes* 51(Suppl 3):405–413.

Prentki, M., Vischer, S., Glennon, M. C., Regazzi, R., Deeney, J. T., Corkey, B. E., 1992. Malonyl-CoA and long chain acyl-CoA esters as metabolic coupling factors in nutrient-induced insulin secretion. *J Biol Chem* 267(9): 5802-10.

Rahier, J., Guiot, Y., Goebbels, R.M., Sempoux, C., Henquin, J.C. 2008. Pancreatic  $\beta$ -cell mass in European subjects with type 2 diabetes. *Diabetes Obes Metab* 10(Suppl 4):32-42

Rao NM., 2010. Cationic lipid-mediated nucleic acid delivery: beyond being cationic. *Chem Phys Lipids*. 163(3):245-52. Epub 2010 Jan 12.

Roberts, L., 1998. Human gene transfer test approved. *Science* 243: 473

Robbins PD, Ghivizzani SC. 1998. Viral vectors for gene therapy. *Pharmacol Ther.*(1):35-47.

Ronnebaum, S. M., Ilkayeva, O., Burgess, S. C., Joseph, J. W., Lu, D., Stevens, R. D., Becker, T. C., Sherry, A. D., Newgard, C. B., Jensen, M. V., 2006. A pyruvate cycling pathway involving cytosolic NADP-dependent isocitrate dehydrogenase regulates glucose-stimulated insulin secretion. *J Biol Chem* 281(41): 30593-602.

Ronnebaum SM, Ilkayeva O, Burgess SC, Joseph JW, Lu D, Stevens RD, Becker TC, Sherry AD, Newgard CB, Jensen MV. 2005. A pyruvate cycling pathway involving NADPH- dependent isocitrate dehydrogenase regulates glucose-stimulated insulin secretion. *J Biol Chem*. 281(41):30593-602.

Ronnebaum, S. M., Jensen, M. V., Hohmeier, H. E., Burgess, S. C., Zhou, Y. P., Qian, S., MacNeil, D., Howard, A., Thornberry, N., Ilkayeva, O., Lu, D., Sherry, A. D., Newgard, C. B. 2008. Silencing of cytosolic or mitochondrial isoforms of malic enzyme has no effect on glucose-stimulated insulin secretion from rodent islets. *J Biol Chem* 283(43): 28909-17.

Sato, Y., Aizawa, T., Komatsu, M., Okada, N., Yamada, T., 1992. Dual functional role of membrane depolarization/Ca<sup>2+</sup> influx in rat pancreatic B-cell. *Diabetes* 41(4):438-43.

Staples, B. J., 2004. Ultrasonic drug delivery--a general review. *Expert Opinion on Drug Delivery*, 1(1), 37-56.

Straub SG., Sharp GW., 2001. Glucose-stimulated signalling pathways in biphasic insulin secretion. *Diabetes Metab Res Rev.* 18(6):451-63.

Shapiro, A. M., Lakey, J., Ryan, E., Korbitt, G., Toth, E., Warnock, G., Kenteman, N., Rajotte R., 2000. Islet transplantation in seven patients with type 1 diabetes mellitus using a glucocorticoid-free immunosuppressive regime. *N.Engl J Med.*, 343(4):230-238.

Shapiro, A. M., Ricordi, C., Hering, B. J., Auchincloss, H., Lindblad, R., Robertson, R. P., Secchi, A., Brendel, M. D., Berney, T., Brennan, D. C., Cagliero, E., Alejandro, R., Ryan, E. A., DiMercurio, B., Morel, P., Polonsky, K. S., Reems, J. A., Bretzel, R. G., Bertuzzi, F., Froud, T., Kandaswamy, R., Sutherland, D. E., Eisenbarth, G., Segal, M., Preiksaitis, J., Korbitt, G. S., Barton, F. B., Viviano, L., Seyfert-Margolis, V., Bluestone, J., Lakey, J. R. International trial of the Edmonton protocol for islet transplantation., 2006. *N.Engl J Med.*, 355:1318-1330.

Shimoda. M., Chen, S., Noguchi. H., 2010. In vivo non-viral gene delivery of human vascular endothelial growth factor improves revascularisation and restoration of euglycaemia after human islet transplantation into mouse liver. *Diabetologia*

Roberts, L., 1989. Human gene transfer test approved. *Science* 243: 473

Robbins, P.D., Ghivizzani, S.C., 1998. Viral Vectors for Gene Therapy. *Pharmacol. Ther. Vol. 80, No.1, pp. 35-47.*

Samols, E., Bonner-Weir, S., 1986. Intra-islet Insulin-Glucagon-Somatostatin Relationships. *Clinics in Endocrinology and Metabolism--Vol. 15, No. 1.*

Samols, E., Stagner, JI, Ewart, RB, Marks, V., 1998. The order of islet microvascular cellular perfusion in the perfused rat pancreas. *J Clin Invest* 82:350-3.

Scheller, E. L., Krebsbach, P.H., 2009. Gene Therapy: Design and Prospects for Craniofacial Regeneration. *J Dent Res* 88(7):585-596.

Sek-Wen Hui., 2008. Overview of Drug Delivery and Alternative Methods to Electroporation. *Methods in Molecular Biology, Vol. 423. 91-107*

Shimoda, M., Chen, S., Noguchi, H., Matsumoto, S., 2010. In vivo non-viral gene delivery of human vascular endothelial growth factor improves revascularisation and restoration of euglycaemia after human islet transplantation into mouse liver. *Diabetologia*

Simberg, D., Danino, D., Talmon, Y., Minsky, A., Ferrari, M. E., Wheeler, C. J., 2003. Phase behavior, DNA ordering and size instability of cationic lipoplexes: Relevance to optimal transfection activity. *Journal of Liposome Research*, 13(1), 86-87.

- Stagner, JI, Samols, 1992. The vascular order of islet cellular perfusion in the human pancreas. *Diabetes* 41:93.
- Stock, P. G., & Bluestone, J. A., 2004. Beta-cell replacement for type I diabetes. *Annual Review of Medicine*, 55, 133-156.
- Straub, S. G., & Sharp, G. W. G., 2002. Glucose-stimulated signaling pathways in biphasic insulin secretion.
- Szabadkai, G., Duchon, M.R., 2009. Mitochondrial mediated cell death in diabetes. *Apoptosis* 14:1405-1423.
- Taplin, C. E., & Barker, J. M., 2008. Autoantibodies in type 1 diabetes. *Autoimmunity*, 41(1), 11-18.
- Thatte, S., Datar, K., & Ottenbrite, R. M., 2005. Perspectives on: Polymeric drugs and drug delivery systems.
- Tinkov, S., Berkerendjian, R., Winter, G., Coester, C., 2008. Microbubbles as Ultrasound Triggered Drug Carriers. *Journal of Pharmaceutical Sciences*, Vol. 98. No. 6 pg 1935-1954.\*\*\*\*\*
- Tong, Q.Ye, C. McCrimmon, R. J. Dhillon, H. Choi, B. Kramer, M. D. Yu, J. Yang, Z. Christiansen, L. M. Lee, C. E. Choi, C. S. Zigman, J. M. Shulman, G. I. Sherwin, R. S. Elmquist, J. K. Lowell, B. B., Tros de Ilarduya C, Sun Y, Düzgüneş N. 2010. Gene delivery by lipoplexes and polyplexes. *Eur J Pharm Sci*.40(3):159-70. Epub 2010 Mar 30.
- Tranchant, I., Thompson, B., Nicolazzi, C., Mignet, N., & Scherman, D., 2004. Physicochemical optimisation of plasmid delivery by cationic lipids. *JOURNAL OF GENE MEDICINE*, 6, S24-S35.
- Unger, E. C., Hersh, E., Vannan, M., & McCreery, T., 2001. Gene delivery using ultrasound contrast agents. *ECHOCARDIOGRAPHY-A JOURNAL OF CARDIOVASCULAR ULTRASOUND AND ALLIED TECHNIQUES*, 18(4), 355-361.
- Unger, R.H., Dobbs, R.E., 1978. Insulin, Glucagon, and somatostatin secretion in the regulation of metabolism. *Ann. Rev. Physiol.* 40:307-43
- Wang, J., Wu, C., Zhang, C., Qiu, Q., Zheng., M., 2008. Ultrasound-mediated microbubble destruction facilitates gene transfection in rat C6 glioma cells. *Mol Biol Rep*, 36:1263-1267
- Wang Z., Thurmond DC., 2009. Mechanisms of biphasic insulin granule exocytosis-roles of the cytoskeleton, small GTPases and SNAR proteins. *J Cell Sci*.122(Pt 7):893-903.

- Wasungu, L., & Hoekstra, D., 2006. Cationic lipids, lipoplexes and intracellular delivery of genes. *Journal of Controlled Release*, 116(2), 255-264.
- Wettig SD., Badea I, Donkuru M, Verrall RE, Foldvari M., 2007. structural and transfection properties of anmi-gemini surfactant based nanoparticles. *J Gene Med*. 9(8):649-58.
- Wetting, S., Verral, R. E., Foldvari, M. 2008. Gemini Surfactants: A New Family of Building Blocks for Non-Viral Gene Delivery Systems. *Current Gene Therapy*, (8), 9-23.
- Wiederkehr, A., Wollheim, B., 2009. Minireview: Implication of Mitochondria in Insulin Secretion and Action. *Journal of Endocrinology* 147(6):2643-2649.
- Yingyongnarongkul, B., Radchatawedchakoon, W., Krajarng, A., Watanapokasin, R., & Suksamrarn, A., 2009. High transfection efficiency and low toxicity cationic lipids with aminoglycerol-diamine conjugate. *Bioorganic and Medicinal Chemistry*, 17(1), 176-188.
- Younes, N. A., Nothias, J., & Garfinkel, M. R., 2008. Islet transplantation: The quest for an ideal source. *Annals of Saudi Medicine*, 28(5), 325-333.
- Zhao, C. Wilson, M. C. Schuit, F. Halestrap, A. P. Rutter, G. A., 2001. Expression and distribution of lactate/monocarboxylate transporter isoforms in pancreatic islets and the exocrine pancreas. *Diabetes*, 50:2 361-6.
- Zhdanov, R.I., Pododed, O.V., Vlassov, V.V., 2002. Cationic lipid-DNA complexes-lipoplexes-for gene transfer and therapy.
- Zhi, D., Zhang, S., Wang, B., Zhao, Y., Yang, B., Yu, S., 2010. Transfection Efficiency of Cationic Lipids with Different Hydrophobic Domains in Gene Delivery. *Bioconjugate Chem*. 21:563-577
- Zhou, X., Liao, Q., PU, Y., Tang, Y., Gong, X., LI, J., XU, Y., Wang, Z., 2009. Ultrasound-mediated microbubble delivery of pigment epithelium-derived factor gene into retina inhibits choroidal neovascularisation. *Chinese Medical Journal* 122(22):2711-2717.
- Zuhorn IS., Hoekstra D., 2002. On the mechanism of cationic amphiphile-mediated transfection. To fuse or not to fuse: is that the question? *J Membr Biol*.189(3):167-79.
- Ziegler, A.G., Nepom, G.T., 2010. Prediction and Pathogenesis in Type 1 Diabetes. *Immunity*, 468-478.